SMALL-SCALE VERTICAL AXIS WIND TURBINE DESIGN

Javier Castillo

ABSTRACT

Tampereen ammatikorkeakoulu

Tampere University of Aplied Sciences

Degree Programme in Aeronautical Engineering

CASTILLO, JAVIER: Small-scale vertical axis wind turbine design

Bachelor's thesis 54 pages, appendixes 15 pages

December 2011

The thesis focuses on the design of a small vertical axis wind turbine rotor with solid wood as a construction material. The aerodynamic analysis is performed implementing a momentum based model on a mathematical computer program.

A three bladed wind turbine is proposed as candidate for further prototype testing after evaluating the effect of several parameters in turbine efficiency, torque and acceleration.

The results obtained indicate that wood is a suitable material for rotor construction and a further development of the computer algorithm is needed in order to improve the flow conditions simulation.

Key words: Wind turbine, giromill, vertical axis, small wind turbine

Table of Contents

1 INTRODUCTION

Wind power energy is getting more shares in the total energy production every year, with wind turbines growing bigger and bigger at the rhythm of technology does.

While we cannot expect nowadays a totally renewal energy supply in Europe, (some estimations say that it is possible for 2030) there are places where energy grid has not even arrived and has not any plans for short or midterm time.

As we charge our mobile phone in any socket, there are people that has to illuminate their homes with kerosene lamps, students that cannot study when the daylight extinct, medicines that cannot be stored in a freezer… There are other people that are connected to the grid but still have energy cuts.

For these people, it seems to be cheaper to have a grid connection than to have an independent energy source, reasons for that are that in an isolated installation the energy has to be chemically stored in batteries, with limited lifetime that makes renewal costs comparable to those of a grid connection.

Furthermore, there are places which will not have electricity access, these places coincide with the poorest and isolated rural areas of developing countries, and these people cannot afford the cost of a wind turbine, nor small nor bigger.

Maybe a free turbine design, that anyone with common workshop materials could build, would make a difference in the living conditions of this people. The purpose of this project is to provide an alternative to these people.

2 PRELIMINARY BUSINESS PLAN

A preliminary analysis of the situation of wind turbines used for similar applications is done analyzing the current manufacturers and market situation.

2.1 Product definition

The product is a vertical axis small-scale wind turbine, corresponding to the micro-generation classification of wind turbines, which is less than 1 kW. The aim of the project is to make an affordable turbine, made locally with available materials in developing countries.

There are two different poles in micro-generation markets:

- On one hand we have manufacturers that had invested in a certification program, use ultimate technologies (i.e. electronic controllers or carbon fiber blades) and have a product oriented to developed country consumer.
- On the other hand there are some non-governmental organizations or individuals that build a model from wood, they also construct the generator, but there is no certification process.

The product is intended to be somewhere in the middle of this situation, having raw materials like wood and without a very sophisticated construction process, the idea is to make it constructible with usual and non electrically driven workshop tools.

The IEC 61400 Wind turbine generator systems standards are the reference used for the certification of wind turbines. The IEC61400-2 focuses in design requirements for small wind turbines but they are not applicable to vertical-axis wind turbines (Wood, 2011).

Technical standards should be considered in the design in order to ensure safety, reliability and durability of the wind turbine, but standards for vertical-axis wind turbines have not been developed and a complete certification should be done by accredited institutions, which is expensive (Cace, et al., 2007).

2.2 Demand analysis

1.6 billion People, 80% of them living in Sub-Saharan Africa and South Asia, do not have access to electricity. This population uses kerosene and batteries for

their households and diesel generators for their businesses (Legros, Havet, Bruce, & Bonjour, 2009).

Access to energy closely correlates with poverty: insufficient access to electricity or other energy sources also means that health services, access to clean water and sanitation, and education all suffer (Cheikhrouhou, 2011).

With scarcity of resources, efforts on grid extension are focused to serve large population cities while rural remote areas are considered to have too much electrification costs to serve few people.

According to (winafrique, 2011):

- A small wind turbine production facility will cost less than a photovoltaic factory of the same capacity.
- Wind turbines are very difficult to develop but not to manufacture.
- Local manufacturing, under license or through a joint venture, is necessary if widespread utilization is to be pursued.

A small wind turbine design with very low regular maintenance, available spare parts and with local users trained could meet the requirements needed for a long operation in developing countries.

The following figure shows the geographical distribution of the areas that could need the product.
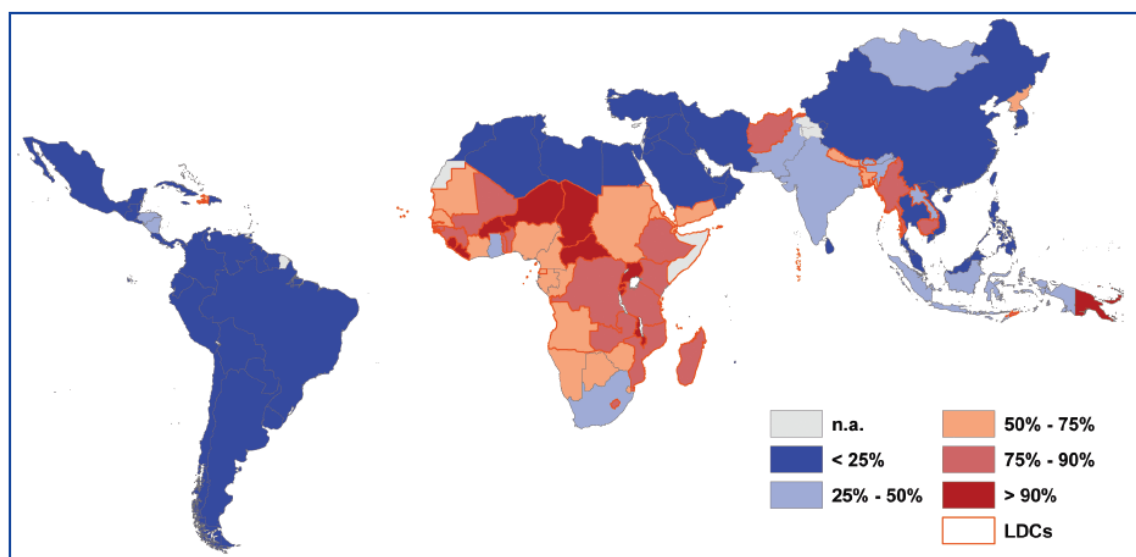
N.A. = not available.

Figure 1. Energy access percentage in developing countries (Legros, Havet, Bruce, & Bonjour, 2009)

2.3 Demand projection

Developing countries have potential demand for small wind systems because they normally do not have electricity grid in rural areas. People need financial assistance to buy small wind systems but government assistance is directed nowadays to subsidizing extension of the grid and installing diesel generators (American Wind Energy Association, 2002).

World electricity generating capacity is projected to increase a 46 percent by 2035, being the non-OECD countries the ones with a major contribution in total capacity increase (71%). The figures on appendix 2, made with extracted data from (U.S. Energy Information Administration, 2011), show the projected increase in wind-powered installed generating capacity by 2035, which will be 2,75 times the actual generating capacity and will represent a 7.37% in the world total generating capacity (nowadays represents the 3,95%).

The use of batteries and subsequent charging is becoming popular as a solution to the lack of electricity in small rural areas. Households in Sri Lanka use automobile batteries to power radio and TV sets. The number of such batteries is claimed to be 300,000. However, recharging the battery takes both time and money (Dunnett).

2.4 Offer analysis

For the present offer analysis, a small wind turbine database has been used (allsmallwindturbines.com, 2011) to compare those models that were more similar to the original idea, which is a vertical axis wind turbine with less than 1 kW of rated power.

From this database we can extract that from the 558 models of wind turbines listed, the 20% was of vertical axis type (VAWT from now on) and the other part was of horizontal axis type (HAWT).

As price was not always available, some contacts with the wind turbine manufacturers have been made. A comparison between some wind turbines is in competence analysis table (see appendix 4).

Another issue was the stated power, there are some studies made in Netherlands and UK that show quite difference between what is stated in the turbine performances and what is really giving (Encraft, 2009).

Manufacturer's characteristics

Approximately 250 companies in the world manufacture, or plan to manufacture, small wind turbines. Of these (American Wind Energy Association, 2002):

- 95 (36%) are based in the United States
- At least 47 (12 U.S.) have begun to sell commercially
- 99% have fewer than 100 employees
- They are spread per 26 different countries
- The vast majority are in start-up phases and roughly half the world market share is held by fewer than 10 U.S. manufacturers.

The Largest Manufacturers in 2009 were:

Table 1. Largest manufacturers considering sales in power installed (American Wind Energy Association, 2002)

Company	Country	kW Sold Worldwide
Southwest Windpower	U.S.	11700
Northern Power Systems	U.S.	9200
Proven Energy	U.K. (Scotland)	3700
Wind Energy Solutions	Netherlands	3700
Bergey WindPower Co.	U.S.	2100

From this five, Bergey Windpower models are being used for rural areas electrification projects in developing countries, some of their projects are:

- Installation in 1998 of three 1.5 kW and one 7.5 kW turbine at a cyclone shelter in Charduani, Bangladesh

- Installation in 1995 of a 1.5 kW turbine for water pumping to Assu, a remote village of 500 people in Brazil.

- One problem, which is common in these types of pioneering projects, is that technical support is based 600 km away in a big city. With only a few systems in the Assu area it is not economically feasible to maintain a support structure closer to the projects, particularly since support is seldom needed. The emphasis, therefore, is placed on making the systems as reliable and maintenance-free as possible.

- Installation on 2005 of a 7.5 kW turbine for powering a cell phone provider station, this resulted in collaboration with winafrique which supplies its products.

- Installation on 1990 of a 10 kW for irrigation purposes in Timbuktu, Mali.

- Installation on 1992 of a 1.5 kW turbine for small-scale irrigation in Oesao, on the island of Timor in East Indonesia.

Bergey Windpower turbines are not perceived as a competitor but as a model to follow; its prices are still unaffordable for the vast majority of people living in remote areas. Their models, with few moving parts and very well proven and designed had achieved a reputation of dependable and reliable in these applications.

Another existing offer is that provided by some organizations like V3power in the UK who make handmade wind turbines courses along Europe, they don't seem to have a direct contact with developing countries or NGOs. They use a model designed by Hugh Piggot, who has been involved in projects in Peru and Sri Lanka among others and has written a "recipe book" to build a wind turbine with common workshop tools and materials.

V3power also sell Hugh Piggot's model prices ranging 1293 $ the 1.2 m diameter turbine to the 2716 $ the 4.2 m rotor, power rating not mentioned. These prices, approximately half value of Bergey Wind Turbines make them more affordable.

This idea of making a wind turbine construable in developing countries without advanced tools and skills coincides with the idea of the project. However it seems to be usual to found cracked or faulty wood blades after storms.

To sum up, the position of the project is intended to be between the reliable, well-proven market turbines and the DIY (Do It Yourself) not standardized models. The intention of the project is to have a viable alternative to those models.

3 WIND TURBINE TYPES

Wind turbines can be classified in a first approximation according to its rotor axis orientation and the type of aerodynamic forces used to take energy from wind. There are several other features like power rating, dimensions, number of blades, power control, etc. that are discussed further along the design process and can also be used to classify the turbines in more specific categories.

3.1 Rotor axis orientation

The major classification of wind turbines is related to the rotating axis position in respect to the wind; care should be taken to avoid confusion with the plane of rotation:

- Horizontal Axis Wind Turbines (HAWT): the rotational axis of this turbine must be oriented parallel to the wind in order to produce power. Numerous sources claim a major efficiency per same swept area and the majority of wind turbines are of this type.

- Vertical Axis Wind Turbines (VAWT): the rotational axis is perpendicular to the wind direction or the mounting surface. The main advantage is that the generator is on ground level so they are more accessible and they don't need a yaw system. Because of its proximity to ground, wind speeds available are lower.

One interesting advantage of VAWTs is that blades can have a constant shape along their length and, unlike HAWTs, there is no need in twisting the blade as every section of the blade is subjected to the same wind speed. This allows an easier design, fabrication and replication of the blade which can influence in a cost reduction and is one of the main reasons to design the wind turbine with this rotor configuration.

3.2 Lift or Drag type

There are two ways of extracting the energy from the wind depending on the main aerodynamic forces used:

- The drag type takes less energy from the wind but has a higher torque and is used for mechanical applications as pumping water. The most representative model of drag-type VAWTs is the Savonius.
- The lift type uses an aerodynamic airfoil to create a lift force, they can move quicker than the wind flow. This kind of windmills is used for the generation of electricity. The most representative model of a lift-type VAWT is the Darrieus turbine; its blades have a troposkien shape which is appropriate for standing high centrifugal forces.

The design idea is to make a lift type turbine, with straight blades instead of curved. This kind of device is also called giromill and its power coefficient can be higher than the maximum possible efficiency of a drag type turbine, like Savonius (Claessens, 2006).

3.3 Power control

The ability to control the power output as well as stand worst meteorological conditions can be achieved passively with stall control or active with pitch control; the majority of small wind turbines use stall control in addition to some blocking device, the NACA44 series airfoils are considered particularly useful for this type of control (Jha, 2011, p. 263) but they will not be used for the cur-

rent design because there is not available data about its behavior depending on the angle of attack.

The Stall control is a passive control which provides overspeed protection, the generator is used to electrically control the turbine rotational speed, when the rated conditions are surpassed (i.e. in a windy storm).

This kind of control mechanism should be the one appropriate for a simple, reliable and low maintenance design because it doesn't add any moving part to the structure nor its associated bearings, which can affect the final cost of the turbine.

The Variable pitch control is achieved by varying actively the pitch (orientation) of the blade in such a way it can adapt to the current airflow speed to take the maximum energy from the wind, its efficiency is increased compared to a fixed pitch windmill and it increases the maximum power that can be extracted from wind. Its main drawback is the need to have a control system to allow these pitch movements. For complex models its worth to have some electronics taking care of that purpose but it is not the case of our design.

3.4 Rotor speed: constant or variable

A constant rotor speed maintains the same rotational speed while the windmill is generating energy; they don't need power electronics to adapt to grid frequency which makes them cheaper; one of their drawbacks is that their optimum efficiency is only achieved at the design airspeed. A stall-regulated wind turbine falls into this category as it maintains constant rpm once the rated rotational speed is achieved.

A variable speed rotor tries to achieve the optimum rotational speed for each wind speed, maintaining constant the optimum tip speed ratio will ensure optimum efficiency at different airspeeds (the concept of tip speed ratio will be developed in section 4.1.3). From a structural point of view, letting the rotor to

change its speed reduces the load supported by the wind turbine in presence of gusts or sudden starts. (Talayero & Telmo, 2008).

3.5 Tower structure

There are two main types of structures, the tube type, which requires low maintenance but higher acquisition costs or the lattice type which is cheaper to build but requires more maintenance. The chosen structure should be related with what is easier and more available to achieve in the community or area of installation.

4 AERODYNAMIC ANALYSIS

In this section, the rotor design parameters are described as well as the model used to calculate its aerodynamic performance. The model limitations are exposed and the computer algorithm and its validation are presented.

4.1 Wind turbine design parameters

The wind turbine parameters considered in the design process are:

- Swept area
- Power and power coefficient
- Tip speed ratio
- Blade chord
- Number of blades
- Solidity
- Initial angle of attack

4.1.1 Swept area

The swept area is the section of air that encloses the turbine in its movement, the shape of the swept area depends on the rotor configuration, this way the swept area of an HAWT is circular shaped while for a straight-bladed vertical axis wind turbine the swept area has a rectangular shape and is calculated using:

$$S = 2R\,L \qquad\qquad [4.1]$$

where S is the swept area [m^2], R is the rotor radius [m], and L is the blade length [m].

The swept area limits the volume of air passing by the turbine. The rotor converts the energy contained in the wind in rotational movement so as bigger the area, bigger power output in the same wind conditions.

4.1.2 Power and power coefficient

The power available from wind for a vertical axis wind turbine can be found from the following formula:

$$Pw = \frac{1}{2}\,\rho\,S\,V_o{}^3 \qquad\qquad [4.2]$$

where V_o is the velocity of the wind [m/s] and ρ is the air density [kg/m^3], the reference density used its standard sea level value (1.225 kg/m^3 at 15ºC), for other values the source (Aerospaceweb.org, 2005) can be consulted. Note that available power is dependent on the cube of the airspeed.

The power the turbine takes from wind is calculated using the power coefficient:

$$C_p = \frac{Captured\ mechanical\ power\ by\ blades}{Available\ power\ in\ wind} \qquad\qquad [4.3]$$

C_p value represents the part of the total available power that is actually taken from wind, which can be understood as its efficiency.

There is a theoretical limit in the efficiency of a wind turbine determined by the deceleration the wind suffers when going across the turbine. For HAWT, the limit is 19/27 (59.3%) and is called Lanchester-Betz limit (Tong, 2010, p. 22). For VAWT, the limit is 16/25 (64%) (Paraschivoiu I. , 2002, p. 148).

These limits come from the actuator disk momentum theory which assumes steady, inviscid and without swirl flow. Making an analysis of data from market small VAWT (see Table 7 from appendix 4), the value of maximum power coefficient has been found to be usually ranging between 0.15 and 0.22.

This power coefficient only considers the mechanical energy converted directly from wind energy; it does not consider the mechanical-into-electrical energy conversion, which involves other parameters like the generator efficiency.

4.1.3 Tip Speed Ratio

The power coefficient is strongly dependent on tip speed ratio, defined as the ratio between the tangential speed at blade tip and the actual wind speed.

$$TSR = \frac{Tangential\ speed\ at\ the\ blade\ tip}{Actual\ wind\ speed} = \frac{R\ \omega}{Vo} \qquad [4.4]$$

where ω is the angular speed [rad/s], R the rotor radius [m] and Vo the ambient wind speed [m/s]. Each rotor design has an optimal tip speed ratio at which the maximum power extraction is achieved. This optimal TSR presents a variation depending on ambient wind speed as will be analyzed on section 5.3.

4.1.4 Blade chord

The chord is the length between leading edge and trailing edge of the blade profile. The blade thickness and shape is determined by the airfoil used, in this

case it will be a NACA airfoil, where the blade curvature and maximum thickness are defined as percentage of the chord.

4.1.5 Number of blades

The number of blades has a direct effect in the smoothness of rotor operation as they can compensate cycled aerodynamic loads. For easiness of building, four and three blades have been contemplated.

As will be illustrated in section 4.3.1, the calculations used to evaluate the power coefficient of the turbine do not consider the wake turbulence effects of the blade, which affect the performance of adjacent blades. The effect of the number of blades will be analyzed further on section 5.5.

4.1.6 Solidity

The solidity σ is defined as the ratio between the total blade area and the projected turbine area (Tullis, Fiedler, McLaren, & Ziada). It is an important non-dimensional parameter which affects self-starting capabilities and for straight bladed VAWTs is calculated with (Claessens, 2006):

$$\sigma = \frac{N\,c}{R} \qquad [4.5]$$

where N is the number of blades, c is the blade chord, L is the blade length and S is the swept area, it is considered that each blade sweeps the area twice. This formula is not applicable for HAWT as they have different shape of swept area.

Solidity determines when the assumptions of the momentum models are applicable, and only when using high σ ≥ 0.4 a self starting turbine is achieved (Tong, 2010).

4.1.7 Initial angle of attack

The initial angle of attack is the angle the blade has regarding its trajectory, considering negative the angle that locates the blade's leading edge inside the circumference described by the blade path. The effect of the initial angle of attack in overall performance will be discussed further on section 5.6.

4.2 Blade performance initial estimations

An initial estimation had to be made to provide guidance in the design process, in order to do that, the extracted data from similar market competitors (see Table 8 from appendix 4) has been analyzed in order to find out reasonable values.

With all this data, an estimation of the required dimensions as well as a rotational speed has been done, as it is not possible to approximate the average wind speed of the whole developing countries, the average wind speed of Tampere has been chosen as this is the location where the possible prototype tests would be conducted. This value has been estimated to be 6 m/s looking at the data provided by (Windfinder, 2011).

Also, it is interesting to have a low value of design wind speed as it will ensure more availability of electrical energy supply with averaged and frequent airspeeds. The turbines found on the market are rated by their maximum power output; this could give false expective on the final user as the rated wind conditions can be higher than the average wind conditions.

Table 2 shows what were the initial estimated performance of the wind turbine, the power coefficient and tip speed ratios had been estimated analyzing the data taken from similar market wind turbines and making an average.

Table 2. Power performance and rotational speed initial estimations for the design wind speed

Power Performance initial estimation			
Design Parameters		Calculated Parameters	
Rotor radius (m)	1	Swept area (m^2)	4
Blade Lenght (m)	2	Solidity	0,8
Blade Chord (m)	0,2		
Power Coefficient	0,17	Rated blade speed (m/s)	12
Tip speed ratio	2	Actual Rotational speed (rad/s)	12
Number of blades	4	Actual Rotational speed (rpm)	114,59
Air constants			
Air density (Kg/m^3)	1,225		
Wind speed (m/s)	6	Power Available from wind (W)	529,2
Conversion factors		**Power output (W)**	**89,964**
rad/s --> rpm	9,54		

4.3 Aerodynamic model

In order to model the performance of a vertical-axis wind turbine there are four main approaches (Cooper, 2010):

- Momentum models
- Vortex models
- Local circulation models
- Viscous models – Computational Fluid Dynamics (CFD)

Each model has its advantages and drawbacks, the main advantage of momentum models is that their computer time needed is said to be much less than for any other approach (Spera, 2009).

Computational fluid dynamics was considered in first place but the time needed for mesh generation in three dimensional analyses was supposed to be too large for the purposes of the present thesis.

The model chosen for the aerodynamic analysis is the double-multiple stream-tube with variable interference factor, often abbreviated DMSV, which is en-

closed in the momentum models category and is based in the conservation of momentum principle, which can be derived from the Newton's second law of motion. It has been used successfully to predict overall torque and thrust loads on Darrieus rotors.
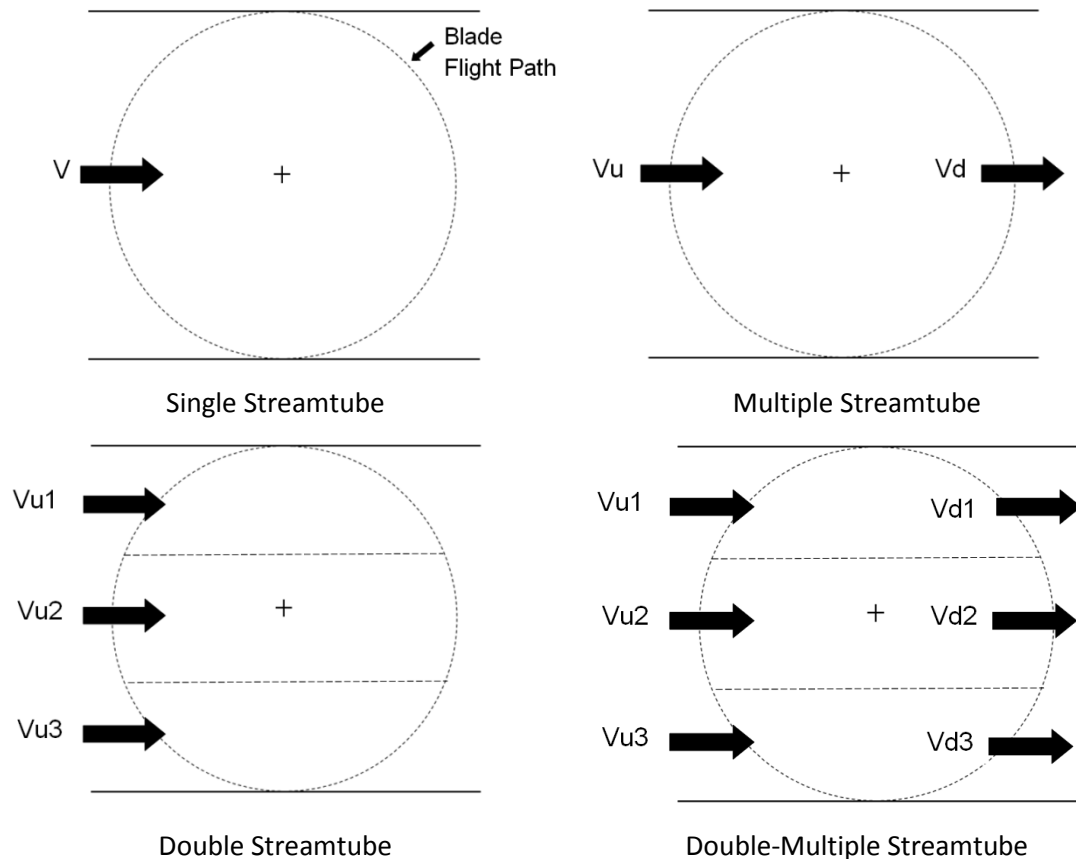

Figure 2. Streamtube models used for vertical-axis wind turbines analyisis, adapted from Spera, 2009, p. 330.

This analytical model was developed by I. Paraschivoiu for determining aerodynamic blade loads and rotor performance on the Darrieus-type wind turbine with straight and curved blades (Paraschivoiu I. , 2002).

The model uses the actuator disk theory, two times, one for the upstream and one for downstream part of the rotor. This theory represents the turbine as a disc which creates a discontinuity of pressure in the stream tube of air flowing through it. The pressure discontinuity causes a deceleration of the wind speed, which results in an induced velocity.

4.3.1 Aerodynamic model explanation

The swept volume of the rotor is divided into adjacent, aerodynamically inde-pendent, streamtubes; each one is identified by his middle θ angle, which is defined as the angle between the direction of the free stream velocity and the position of the streamtube in the rotor (see Figure 3).

The analysis of the flow conditions is made on each streamtube using a combi-nation of the momentum and blade element theories, the former uses the con-servation of the angular and linear momentum principle and the later divides the blade in N elements and analyzes the forces on the blades (lift and drag) as a function of blade shape. Further details on blade element momentum theory can be found on Manwell, McGowan and Rogers, 2009, p. 117-121.

It is assumed that the wind velocity experiments a deceleration near the rotor, if we represent the front and rear part of the turbine by two disks in series, the velocity will be decelerated two times, one for the upstream and the other for the downstream.

Unlike for the analysis of a troposkien shaped Darrieus turbine, it has been as-sumed no vertical variation of the induced velocity as a straight vertical blade is subjected to the same flow velocity along its length.
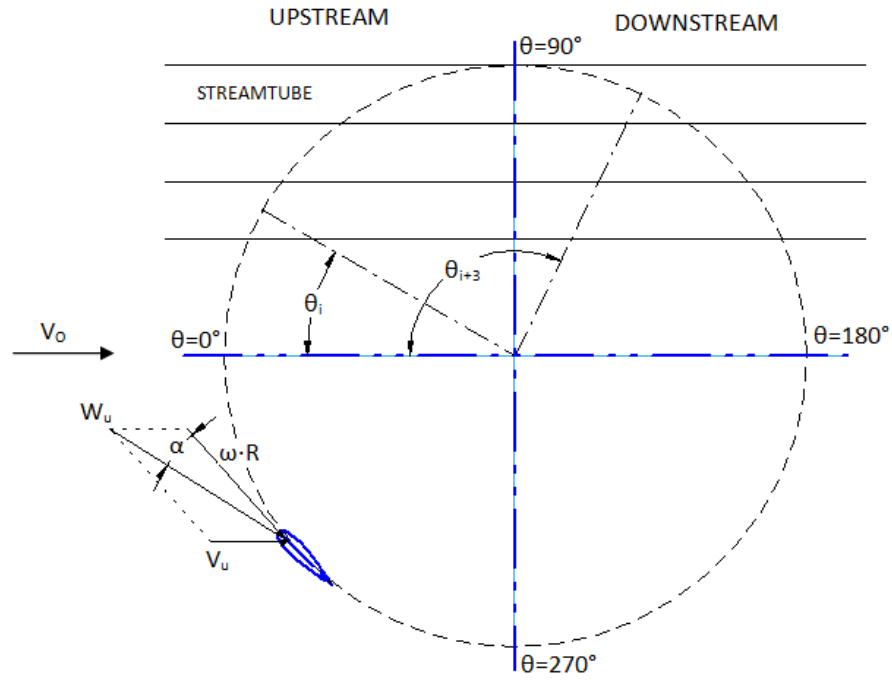
Figure 3. Division of the rotor swept area into streamtubes, definition of velocities and angles.

According to Paraschivoiu (2002) the induced velocities decrease in the axial streamtube direction in the following manner:

The induced velocity in the upstream part of the rotor is:

$$Vu = \text{Vo } au \qquad [4.6]$$

where *Vu* is the upstream induced velocity, Vo is the free stream air velocity and *au* is the upstream interference factor, which is less than 1 as the induced velocity is less than the ambient velocity.

In the middle plane between the upstream and downstream there is an equilibrium-induced velocity Ve:

$$Ve = \text{Vo } (2\ au - 1) \qquad [4.7]$$

Finally, for the downstream part of the rotor, the corresponding induced velocity is:

$$Vd = Ve\ ad \qquad [4.8]$$

where *Vd* is the downstream induced velocity and *ad* is the downstream interference factor which is smaller than the upstream interference factor.

Knowing the induced velocities all around the blade trajectory will allow us to calculate the lift and drag forces associated to every blade position and then,

these forces can be related to the torque and power coefficient produced by the wind turbine.

The resultant air velocity that the blade sees is dependent on the induced velocity and the local tip speed ratio:

$$Wu = \sqrt{Vu^2 \left[(TSR - \sin^2\theta)^2 + (\cos^2\theta)\right]} \qquad [4.9]$$

where Wu is the resultant air velocity and TSR is the local tip speed ratio defined as:

$$TSR = R\,\frac{\omega}{Vu} \qquad [4.10]$$

where R is the rotor radius and ω is the angular speed.

The resultant air velocity is used then to determine the local Reynolds number of the blade.

$$Re_b = \frac{Wu\,\text{c}}{\text{K}_v} \qquad [4.11]$$

Where Re_b is the local Reynolds number, c is the blade chord and K_v is the kinematic viscosity of the air, which has a reference value of 1.4607e-5 [m^2/s] for an air temperature of 15ºC (Aerospaceweb.org, 2005).

The equation for the angle of attack of the blade has been taken from Paraschivoiu (2002), the result has been demonstrated in order to ensure what is considered the 0º of the azimuth angle (θ) and also what is considered a negative angle of attack.

$$\alpha = \arcsin\left(\frac{\cos\theta\,\cos\alpha_0 - (X - \sin\theta)\,\sin\alpha_0}{\sqrt{\left[(TSR - \sin^2\theta)^2 + (\cos^2\theta)\right]}}\right) \qquad [4.12]$$

where α is the angle of attack which is defined as the angle between the blade chord and the resultant air velocity vector.

The previous equation allows the introduction of an initial angle of attack α_0 different from 0º. It considers positive angles of attack those which have the relative wind speed vector outside the rotor as in Figure 3, which occurs in the whole upstream half of the rotor.

Two different more intuitive formulas can be used to calculate the angle of attack at each blade position.

$$\alpha_{righthalf} = \arctan\left(\frac{Vu \, \cos\theta}{\omega \, R + Vu \, \sin\theta}\right) \qquad [4.13]$$

$$\alpha_{lefthalf} = \arctan\left(\frac{Vu \, \cos\theta}{\omega \, R - Vu \, \sin\theta}\right) \qquad [4.14]$$

The local Reynolds number and the angle of attack are then used to find the corresponding lift and drag coefficients using double interpolation (i.e. one interpolation for the Reynolds number and another for the angle of attack). The data tables had been extracted from Sheldahl and Klimas (1981).

The variation of lift and drag coefficients depending on Reynolds number is only patent while α<30⁰ (see Figure 4), then all the curves converge. This is because the data is a joint between experimental data until 30⁰ and computed data with an airfoil synthesizer code.
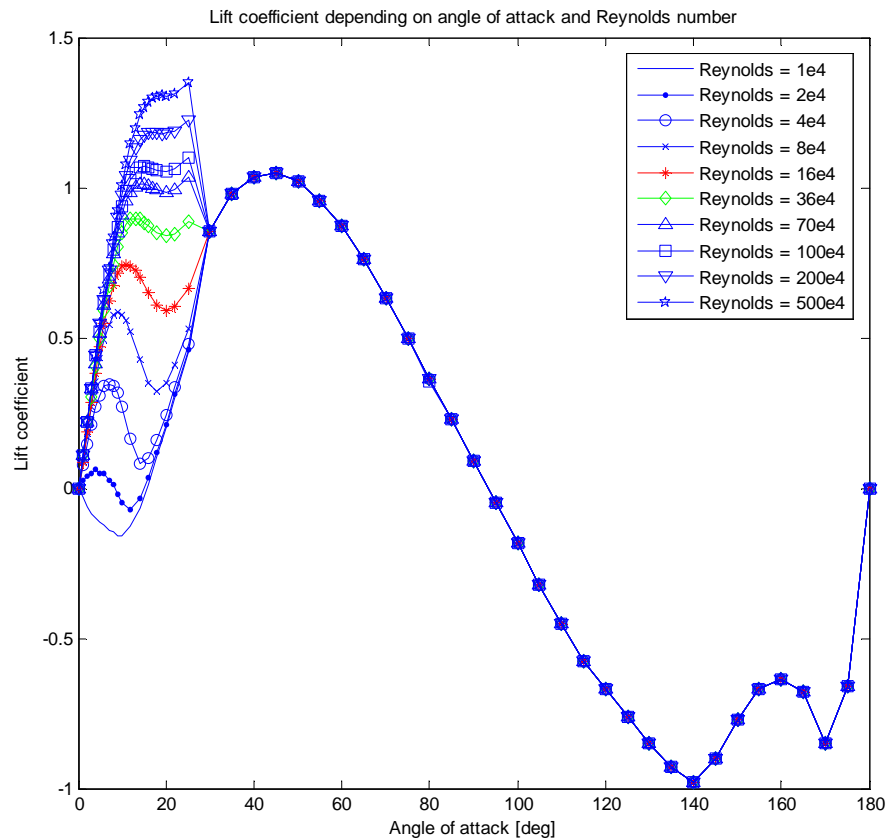

Figure 4. Lift coefficient variation with Reynolds number

The existing step between the two types of data has been considered a problem for a smoother simulated torque behavior, but a close analysis at the Reynolds number involved in the calculations for the design wind speed of 6 m/s has shown that the Reynolds ranges between $16 \cdot 10^4$ (in green) and $36 \cdot 10^4$ (in red) which have a smoother transition.

Furthermore, the range of angle of attack variation becomes smaller as the tip speed ratio increases; this can be appreciated in the following simulation of the angle of attack variation of a blade in a full revolution:
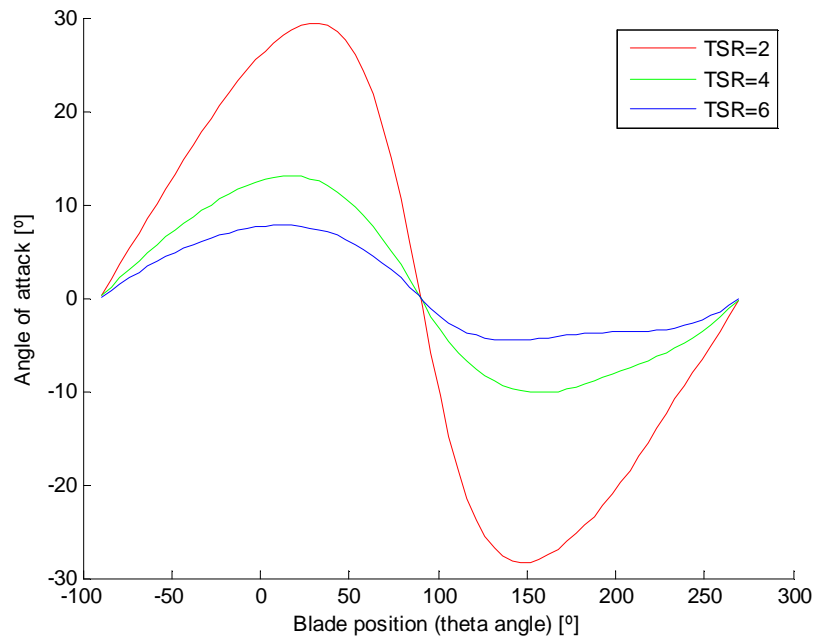

Figure 5. Angle of attack variation in a blade revolution for different tip speed ratios.

For the purpose of calculating the torque produced by the blade, the lift and drag forces are split in a blade trajectory tangential component and a normal component (radial).

The normal and tangential coefficients can be calculated using:

$$Cn = Cl \, \cos \alpha + Cd \, \sin \alpha \qquad [4.15]$$

$$Ct = Cl \, \sin \alpha - Cd \, \cos \alpha \qquad [4.16]$$

where Cn and Ct are the normal and tangential coefficients respectively and Cl and Cd are the lift and drag coefficients.

According to Paraschivoiu, using the blade element theory and the momentum equation, the upwind flow conditions can be characterized by f_{up}:

$$fup = \frac{N\,c}{8\,\pi\,R} \int_{-\frac{\pi}{2}}^{\frac{\pi}{2}} |\sec\theta|\ (Cn\,\cos\theta - Ct\,\sin\theta)\ d\theta \qquad [4.17]$$

where N is the number of blades.

Then the interference factor can be obtained by:

$$au = \frac{\pi}{fup + \pi} \qquad [4.18]$$

For a given rotor geometry, rotational speed and free stream velocity, a first set of calculations from equations 4.6 to 4.18 is made using au=1, then with the new value of au the procedure is repeated until the initial and final au value are similar. This is repeated for each streamtube position and once the upstream induced velocities have been calculated, the downstream half is calculated using the same set of formulas, interchanging the upstream induced velocity Vu by the downstream induced velocity Vd (see equation 4.8).

4.3.2 Rotor torque and performance

The tangential and normal forces as function of the azimuth angle θ are calculated the same way as lift and drag forces in an airfoil:

$$Fn\,(\theta) = \frac{1}{2}\,\rho\,c\,L\,W^2\,Cn \qquad [4.19]$$

$$Ft\,(\theta) = \frac{1}{2}\,\rho\,c\,L\,W^2\,Ct \qquad [4.20]$$

where Fn and Ft are the normal and tangential force respectively, ρ is the air density [kg/m³], c is the blade chord [m], L is the blade length [m] and W is the relative wind speed.

The Torque produced by a blade is calculated using a combination between the Lift and Torque formulas.

$$Q\,(\theta) = \frac{1}{2}\,\rho\,c\,R\,L\,Ct\,W^2 \qquad [4.21]$$

The average torque produced by the upstream half of the rotor (N/2 blades) is estimated averaging the contributions of each streamtube:

$$Q_{av} = \frac{N}{2\,\pi}\int_{-\frac{\pi}{2}}^{\frac{\pi}{2}} Q(\theta)\,d\theta \qquad [4.22]$$

In order to work with non-dimensional magnitudes the average torque coefficient Cq_{av} is calculated by:

$$Cq_{av} = \frac{Q_{av}}{\frac{1}{2}\,\rho\,Vo^2\,S\,R} \qquad [4.23]$$

And finally the upstream half power coefficient Cpu is calculated with:

$$Cpu = Cqu_{av}\,Xt \qquad [4.24]$$

where Xt is the rotor tip speed ratio which is calculated by:

$$Xt = \frac{R\,\omega}{Vo} \qquad [4.25]$$

The average torque and power coefficient for the downstream half of the rotor are calculated using the same set of formulas from 4.21 to 4.24 using its corresponding values of tangential coefficient and induced velocities.

The total power coefficient of the rotor is calculated then adding the two contributions:

$$Cpt = Cpd + Cpu \qquad [4.26]$$

where Cpt and Cpd are the total and downstream power coefficients respectively.

4.4 Model limitations

4.4.1 Streamtube Expansion Model

The double-multiple streamtube model does not account for expansion of the fluid as it losses velocity. A more realistic model considers the expansion of the streamtube affecting thus the interference factor calculation.

The significance of the streamtube expansion effects is greater as the tip speed ratio increases, being the difference between the power coefficients calculated with the streamtube expansion effect and without it less than 4% beyond a tip speed ratio of 8. The consideration of the expansion effects result in lower loads on the downwind half of the turbine (Paraschivoiu I. , 2002, págs. 194-199).

As the tip speed ratio is designed to be below 3, the streamtube expansion effects will not be included in the calculation as its contribution to the accuracy of the results is not enough relevant.

4.4.2 Dynamic stall

Dynamic stall is an unsteady aerodynamic effect that occurs at low tip speed ratios, due to quick and big variations of the angle of attack a vortex originates on the leading edge of the airfoil; this vortex produces higher lift, drag and pitching moment coefficients than those produced in static stall.

The MDSV code can be modified to include a model to compute these dynamic effects at low speed ratios. A description of the phenomenon as well as the dynamic-stall models that can be used can be found at (Paraschivoiu I. , 2002).

4.5 Algorithm implementation

4.5.1 Algorithm explanation

A Matlab algorithm, included in appendix 5 has been developed using the above described process as a reference to calculate the aerodynamic loads, torque and power coefficient.

The algorithm has as inputs the rotor design parameters, the ambient air velocity and a set of tables containing the airfoil lift and drag coefficients depending on Reynolds number and angle of attack (see figure below). For each streamtube it computes with iteration process the interference factor, relative wind velocity, Reynolds number, angle of attack and tangential and normal forces.
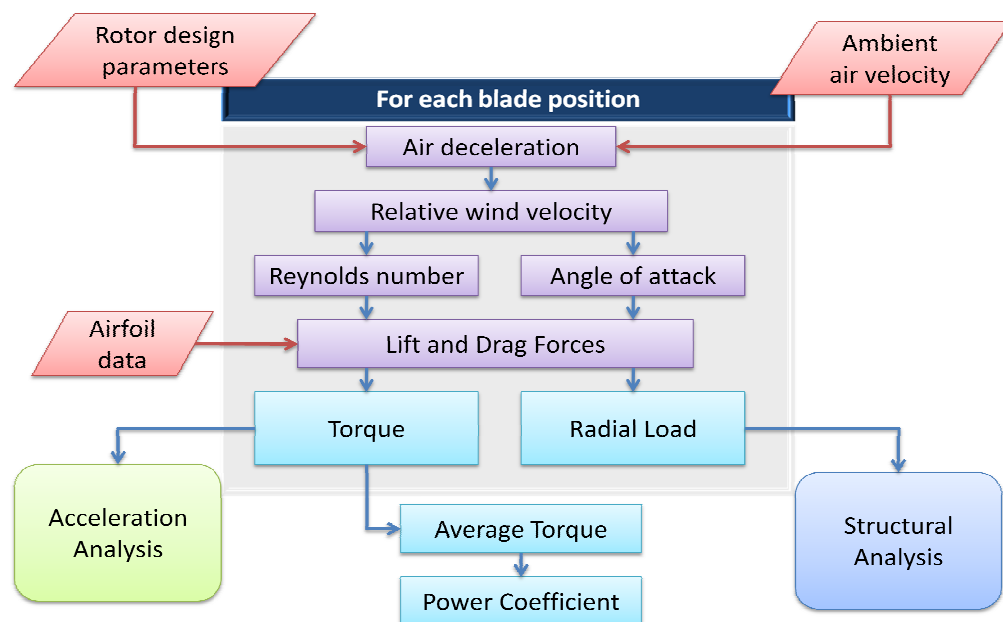

Figure 6. Algorithm schematic diagram

The resulting torque and normal load (radial load) are used then for the acceleration and structural analysis respectively and the torque and power coefficient are obtained by integration of all the blade positions.

4.5.2 Number of streamtubes used

For the whole process, 36 streamtubes had been used, which means evaluating the wind conditions at blade positions in 5^0 increments. This number is the same used by the author of the procedure for presenting the results of his model (Paraschivoiu I. , 2002, p. 164).

A bigger number of streamtubes has been tested to evaluate the air conditions in smaller increments but the resulting power coefficient and torque doesn't present any variation.

4.6. Algorithm validation

The Matlab Algorithm has been validated using the known results of one of the aerodynamic prediction models developed by I. Paraschivoiu. This model called CARDAAV considers the interference factor varying in function of the azimuth angle and also can consider secondary effects.

It should be noted that the reference data was taken reading a plot because the numeric results were unavailable, furthermore the code version CARDAAV which has been used to compute the reference plot consider secondary effects like the rotating tower and the presence of struts, which makes a difference in maximum power coefficient of 6% (Paraschivoiu I. , 2002, p. 185), the developed algorithm gives a difference in maximum Cp of 4.7%.

A comparison between the qualitative accuracy of the algorithm compared with the reference turbine give us a good approximation of the turbine performance at TSRs lower than 3.5, which will be the range of our turbine (see figure 7).

The reference turbine is found on (Paraschivoiu, Trifu, & Saeed, 2009) and its parameters are:

Table 3. Rotor parameters for the 7kW reference turbine (Paraschivoiu, Trifu, & Saeed, 2009)

Parameter	Value
Rotor diameter	6.0 m
Rotor height	6.0 m
Blade length	6.0 m
Blade chord (constant)	0.2 m
Blade airfoil	NACA0015
Number of blades	2
Rotor ground clearance	3 m
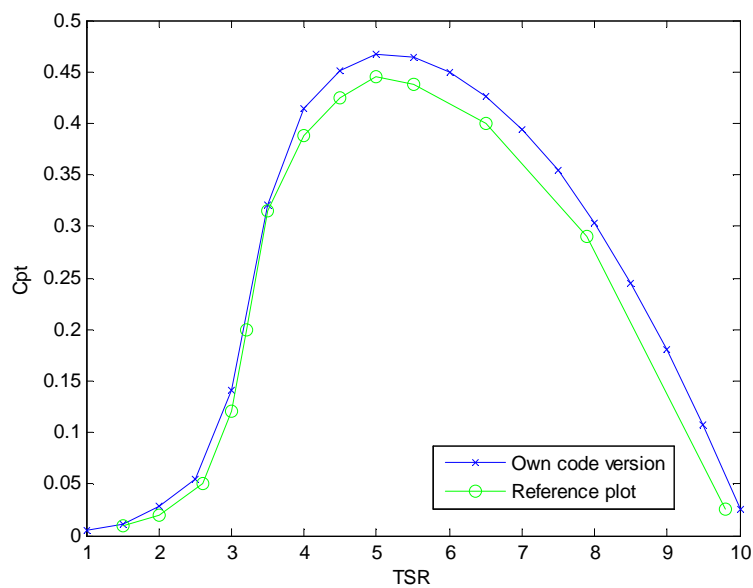
Figure 7. Comparison between own code results and the CARDAAV code, data taken from (Paraschivoiu, Trifu, & Saeed, 2009).

The own version of the aerodynamic model takes into account a varying interference factor in function of the azimuth angle but doesn't consider the following effects that should improve the accuracy of the model:

- Presence of struts and mast.
- Vertical variation of the freestream velocity.
- Expansion of the streamtubes.
- Dynamic stall effects.

A second validation with the results found from computational fluid dynamics and experimental analysis of a small wind turbine has been done in order to see the possible inaccuracy of the model for our design.

The second reference turbine is analyzed on (Raciti Castelli;Englaro;& Benini, 2011) and its parameters are:

Table 4. Rotor parameters for the second reference turbine (Raciti Castelli, Englaro, & Benini, 2011)

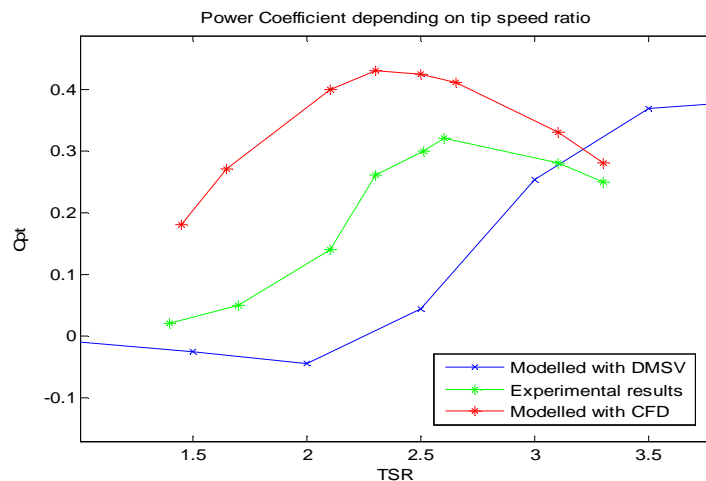| Parameter	Value
Rotor diameter	1.03 m
Blade length	1.4564 m
Blade chord (constant)	0.0858 m
Blade airfoil	NACA 0021
Number of blades	3

Figure 8. Comparison between CFD, DMSV and experimental results, data taken from (Raciti Castelli, Englaro, & Benini, 2011)

We can see that the algorithm is not accurate for small wind turbines at small tip speed ratios, this can be, as noted in (Claessens, 2006), because the momentum based models are limited to solidities below 0.2, for bigger solidities the assumptions of the momentum model are not valid (e.g. homogeneous, incompressible, steady state flow; no frictional drag or non-rotating wake).

Despite these results, the momentum based model is still considered a useful tool in the design process as it gives quicker and qualitative results than other

methods. Different computational options, like CFD, are too time consuming to be considered for use within the scope of this thesis.

5. ROTOR DESIGN

5.1 Starting parameters

A numerical optimization process of the design parameters have been done in order to select which could be the proper parameters for the intended application. The optimization process has been carried out focusing on the effect each parameter has in the power coefficient and torque produced; the results are presented in plots.

In order to speed up the optimization process, some of the parameters have to be fixed for our purposes. The fixed parameters will be the design airspeed and the blade swept area.

The usual power coefficient values shown at the comparison with the competence turbines are between 0.15 and 0.2, so a swept area between 4 and 5.2 m^2 is needed to have 100W at 6 m/s. The selected swept area will be kept to 4 m^2.

The design airspeed is kept at 6 m/s, because the purpose of the application is to take profit of the average wind speed rather than higher speeds, which are not so frequent.

The starting parameters and conditions in which the wind turbine has been tested are shown in table 5:

Table 5. Starting values of the turbine parameters for the optimization process.

Symbol	Parameter	Starting value
Vo	Airspeed	6 m/s
TSR	Tip speed ratio	2
R	Rotor radius	1 m
c	Blade chord	0.3 m
L	Blade length	2 m
N	Number of blades	4
α_o	Initial angle of attack	0^0

5.2 Airfoil selection

The airfoil has been selected considering the availability of airfoil data for angles of attack between -30 and 30^0 and the final thickness of the blade which is associated with its ability to withstand the loads.

The available airfoils with enough data to conduct the study of the aerodynamic loads and behavior of the wind turbine were available in a document issued by Sandia National Laboratories (Sheldahl & Klimas, 1981), this document provides the lift and drag coefficients depending on Reynolds number and angle of attack ranging from 0 to 180^0 for several NACA airfoils.

The selected airfoil is the NACA0021, which aerodynamics characteristics were determined using an airfoil property synthesizer code. This profile is one of the thickest available (21% of chord) and when compared with NACA0015 (thickness is 15% of chord) it can be seen that the self-starting behaviour is improved with thicker airfoils (see Figure 9).
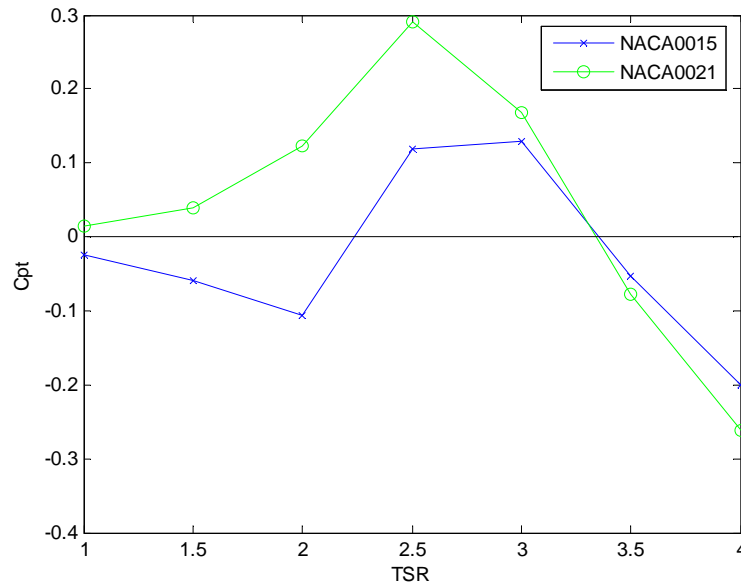
Figure 9. Performance comparison between two different airfoils.

The actual shape of the NACA0021 airfoil can be found at (Abbott & Von Doenhoff, 1959, p. 335); Table 9 from appendix 6 shows the ordinates in percent of chord.

The airfoil selection can be done using an airfoil simulation program like RFOIL, which according to (Claessens, 2006) can have problems to accurately predict the airfoil behavior at Reynolds numbers lower than $1 \cdot 10^6$. Other alternative to wind tunnel testing are the two-dimensional computational fluid dynamics simulations.

5.3 Design airspeed

A modification in the free stream velocity from 0 to 15 m/s varies the power coefficient significantly, beyond this airspeed the power coefficient remains constant at each tip speed ratio as shown in Figure 10.
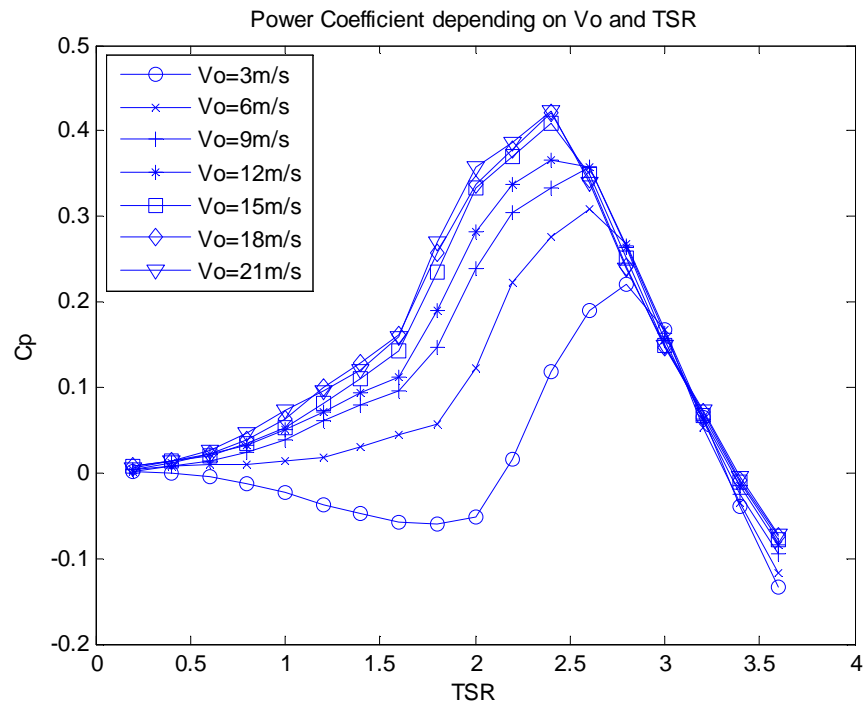
Figure 10. Power coefficient depending on ambient airspeed (Vo) and tip speed ratio (TSR).

The torque behavior increases notably due to its quadratic dependence on air-speed.
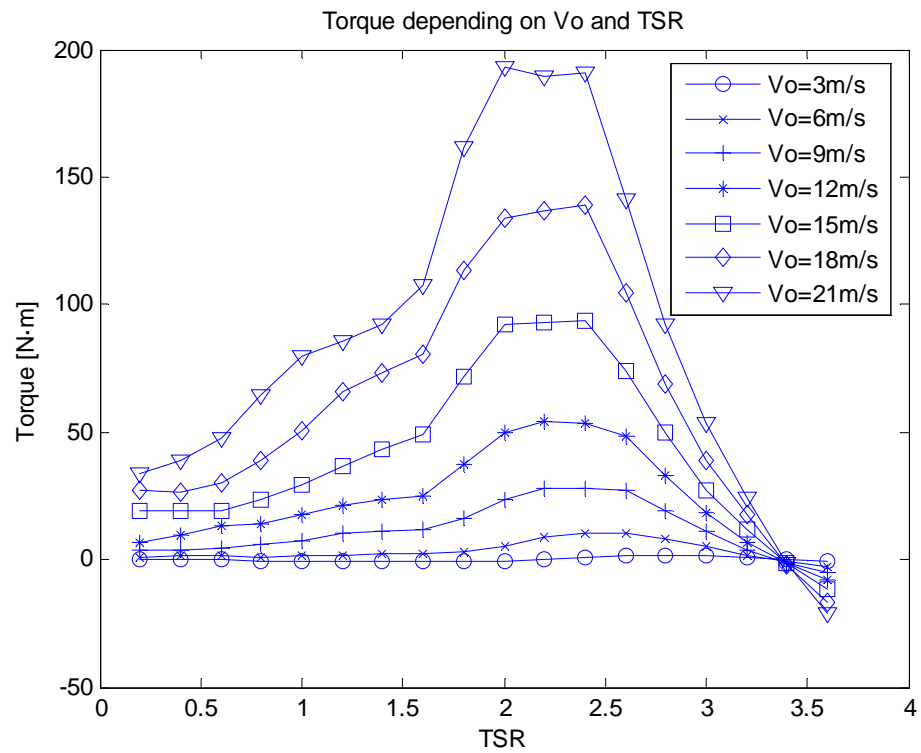

Figure 11. Torque depending on ambient airspeed (Vo) and Tip Speed Ratio (TSR).

The target performance is 100 W at 6 m/s, which should correspond to the rated wind speed, and therefore the maximum rpm of the turbine should be the corresponding to the optimum tip speed ratio of the turbine. But, in order to take advantage also of higher wind speeds, the rated wind speed will be set to 9 m/s but maintaining the initial performance target at 6 m/s.

The usual rated wind speed value ranges from 11.5 to 15 m/s, but a lower value may produce more energy overall because it will be more efficient at wind speeds between cut-in and rated.

5.4 Rotor dimensions

The blade length and rotor radius have a major contribution in the torque behavior of the turbine as can be deduced from the torque equation. In general as bigger these parameters, bigger the torque produced. These parameters are involved also in the solidity calculation. The solidity becomes an important parameter when scaling down or up wind turbines and also determines the applicability of the momentum model.

The radius and blade variation analysis is done maintaining constant swept area. It can be seen in Figure 12 that an increase in rotor radius leads to greater maximum power coefficients, but they are achieved at greater tip speed ratios, so the little the radius, the less tip speed ratio is necessary to work at maximum power coefficient.
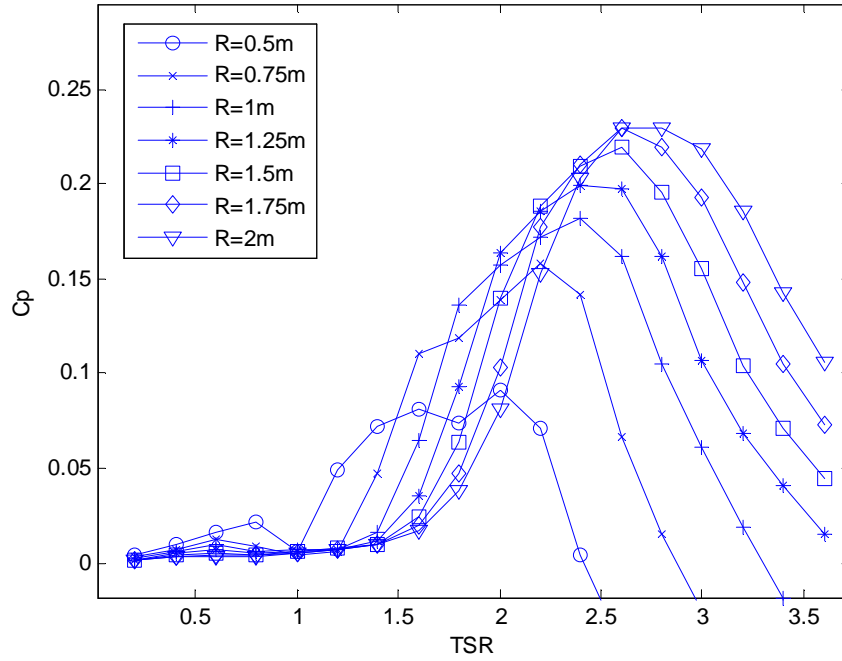
Figure 12. Power coefficient dependent on rotor radius (R) and tip speed ratio (TSR) maintaining constant Swept area.

The power coefficient is not affected by a sole variation of the blade length. This is deduced if the equation for calculating the power coefficient is developed and simplified (Equation 4.24), in this case the upwind power coefficient is illustrated, but the dependences are equal on the downstream half. We can see blade length is present both in the numerator and denominator of the equation.

$$C_{pu} = \frac{N\, c\, \omega\, \int_{-\frac{\pi}{2}}^{\frac{\pi}{2}} C t\, W^2 d\theta}{4\, \pi\, V o^3} \qquad [5.1]$$

The rotor radius R is simplified also from the equation but it is still implicit in the calculation of the relative velocity W, so we can state that the rotor radius have influence both in torque (see figure 13) and power coefficient.

Nevertheless, the torque is affected by the blade length the same way the tangential force coefficient is dependent on the blade surface. Thus the blade length only affects torque and its optimization has to be done considering other factors as the swept area, which determines the power available from wind.

The blade tip losses are not contemplated in the model, in fact, one of the initial assumptions of the model is that there is no interaction between streamtubes,

so in a real model, an increase on blade length should make the blade more efficient.

The optimization needs the input of a fourth factor, the maximum load due to both aerodynamic loads and rotational speed, as the radius will be the one determining them.
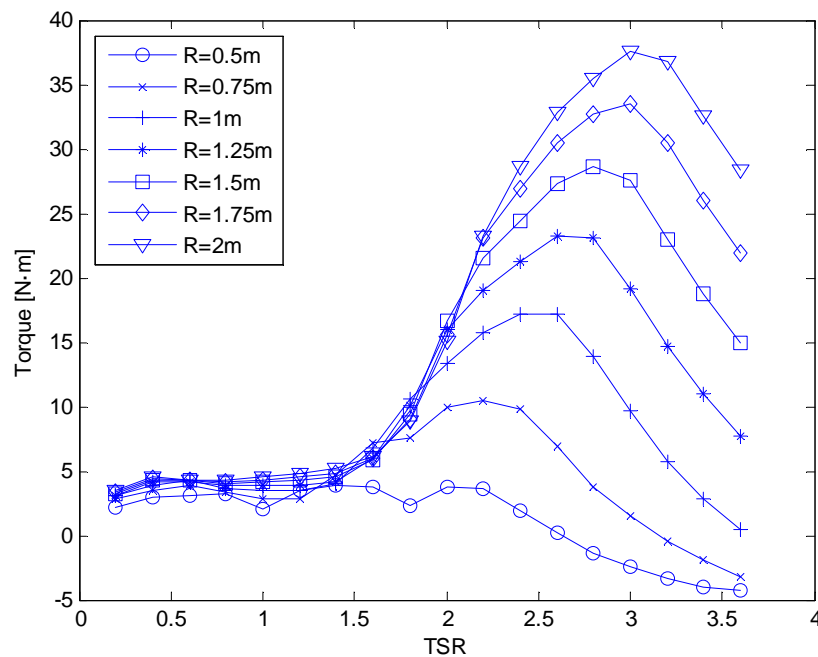
Figure 13. Torque dependent on rotor radius (R) and tip speed ratio (TSR) maintaining constant Swept area.

5.5 Solidity

Solidity is dependent on blade chord, number of blades and rotor radius; as radius effect has been already analyzed for constant swept area, the chord will be analyzed independently.

An increase in blade chord advances the TSR at which the maximum power coefficient is achieved, as bigger the chord, smaller the tip speed ratio. In order to reduce the centrifugal force, a big chord may be more effective than a lighter blade.
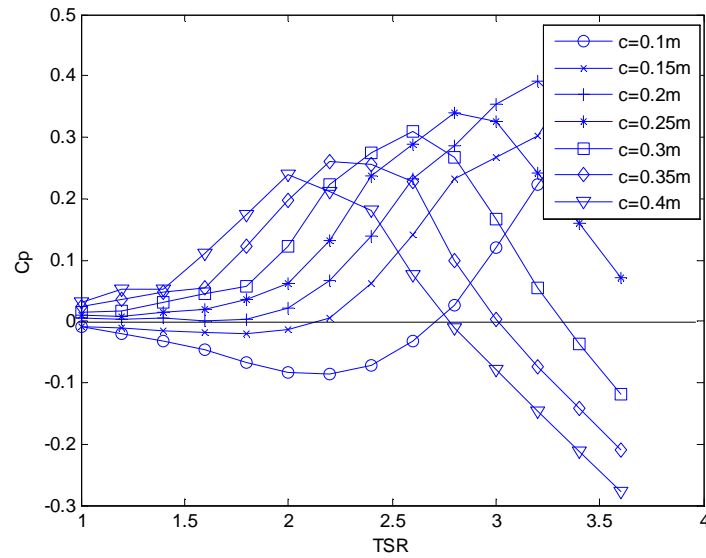
Figure 14. Power coefficient dependent on blade chord (c) and tip speed ratio (TSR).

A bigger chord advances also the point of maximum torque, blades with smaller chords need a bigger tip speed ratio to develop maximum torque and it can affect the self-starting capabilities.

We can anticipate looking at figures 14 and 15 that a carefully decision about the chord length affects self-starting behavior, optimum TSR and maximum power coefficient, so the maximum allowable loads will determine the suitable chord for our model.
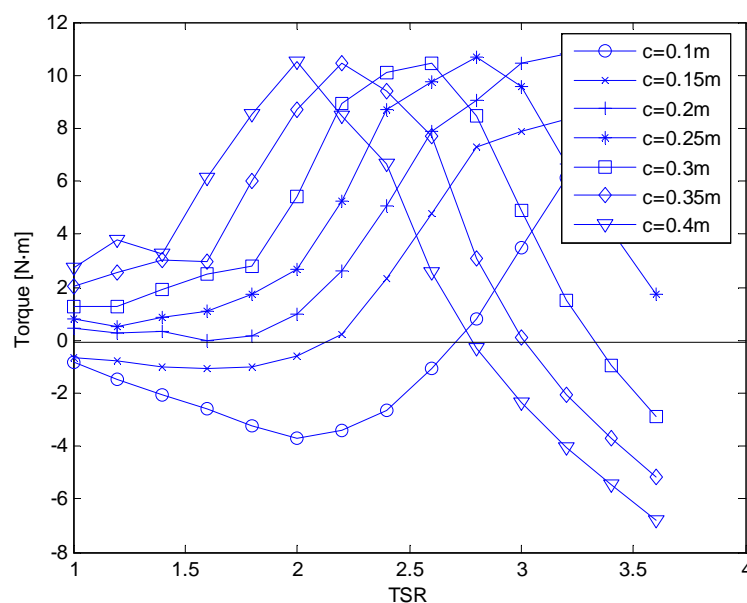
Figure 15. Torque dependent on blade chord (c) and tip speed ratio (TSR).

A better self-starting behavior will allow a smaller cut-in wind speed but will limit the maximum achievable power coefficient; the chord will be selected between 0.25 or 0.3 m depending on their acceleration behavior and structural limits.

The other parameter affecting solidity is the number of blades, keeping in mind the possible interference between blades and also a low solidity value, only three and four-bladed designs will be analyzed. Furthermore, the algorithm doesn't account for the wake turbulence that is created behind each blade and can seriously affect the adjacent blade's lift and drag forces so a big number of blades may give too optimistic results.

Figures 16 and 17 compare the effect of blade number on the power coefficient and average torque. As can be deduced from equations 4.17 and 4.18, a bigger number of blades lead to a bigger deceleration of the air, and this effect is greater than the increase in torque that can be produced having more blades.
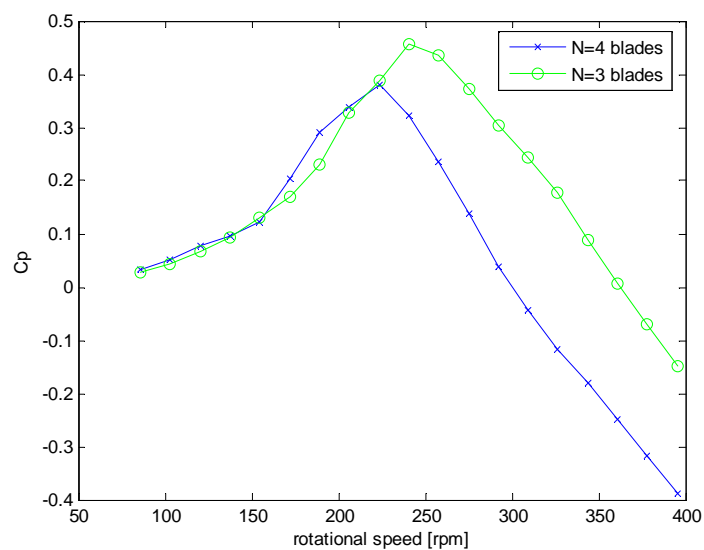
Figure 16. Number of blades effect in power coefficient at several rotational speeds, the two models had blade chords of 0.28 m, NACA0021 airfoils and Vo is 9 m/s.
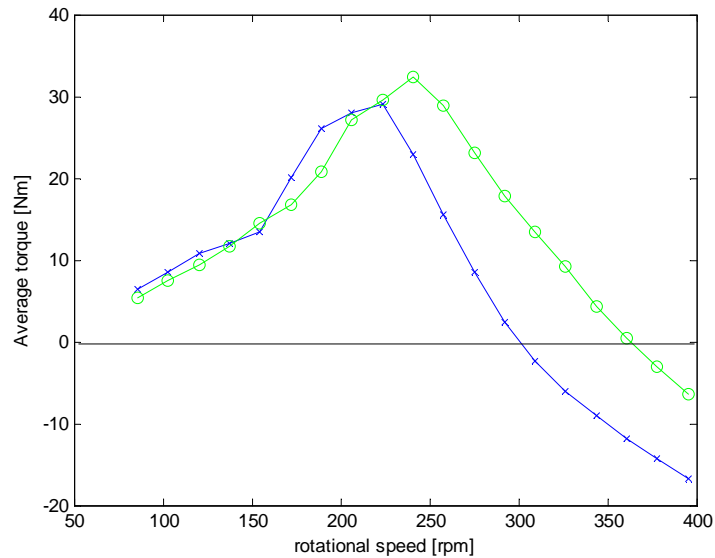
Figure 17. Number of blades effect in average torque at several rotational speeds, the two models had blade chords of 0.28 m, NACA0021 airfoils and Vo is 9 m/s.

In this case, three blades are more efficient than four for the same rotational speed; the final decision will be made considering the acceleration behavior, which will provide a better view of the self-starting characteristics.

5.6 Initial angle of attack

A positive initial angle of attack broadens the range of angular speed operation and a negative one shortens it (see figure 18); this is interesting when fixing the maximum rpm. Furthermore the torque is influenced the same way resulting in a lower maximum power coefficient and torque for negative angles of attack.

The initial angle of attack for our design will be set at 0 degrees as the advantages of a different angle of attack are, according to this model, only evident at higher tip speed ratios than the intended for the model.
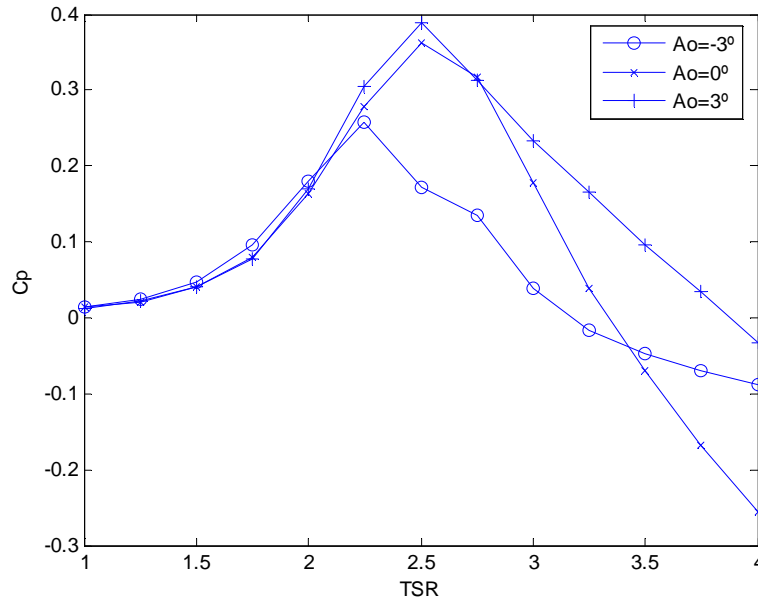
Figure 18. Power coefficient variation depending on the initial angle of attack.

6. ACCELERATION ANALYSIS

An acceleration analysis has been performed in order to ensure the wind turbine will achieve the desired rpm. The first step is to make an estimation of the inertial momentum.

The rotor has been divided in N blades with two beams each, one on the bottom and one on the top. Approximatting the form of the blade to a cuboid and using the Steiner teorem, we have that the inertial moments are:

$$I_{blade} = \frac{1}{12} \, m_{blade}(c^2 + (0.21 \, c)^2) + m_{blade} \, R^2 \qquad [6.1]$$

$$I_{beam} = \frac{1}{12} \, m_{beam}(width^2 + R^2) + m_{blade} \left(\frac{R}{2}\right)^2 \qquad [6.2]$$

where I stands for Inertia moment [kg m^2] and m for mass [kg]. In order to calculate the mass of the wind turbine, a wood density of 500 kg/m^3 is used.

Multiplying the inertial momentum by the number of blades we have an approximate value of the total inertial momentum and we can calculate the angular acceleration:

$$\alpha = \frac{Q}{I} \qquad [6.3]$$

where α is the angular acceleration [rad/s^2], Q the torque [Nm] and I the rotor inertia moment [kg m^2].

A qualitative acceleration analysis has been done (note that blades are approximated to cuboids) between a three-bladed rotor and a four-bladed rotor at a constant airspeed of 25 m/s in order to see if the diminution of inertia moment and different blade arrangement can improve the acceleration characteristics.
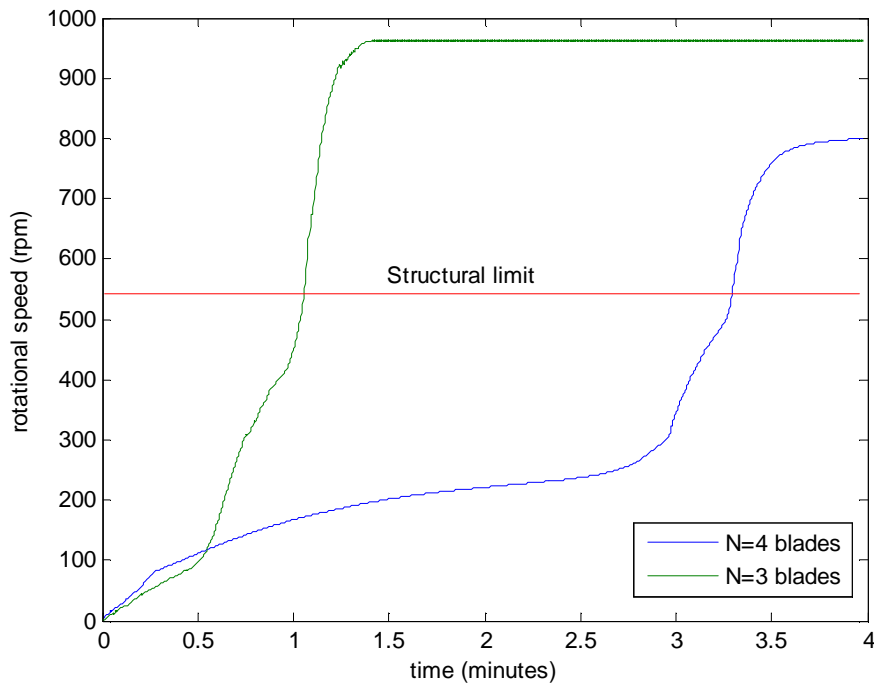
Figure 19. Acceleration analysis of a three and a four-bladed design, at 25 m/s wind speed and chord=0.24.

The four-bladed design has better behavior at low rpm, but the three bladed rotors present a much quicker response, which can be further improved using a lighter material and can be very useful to take profit from brief gusts. The four-bladed rotor will not be further considered in the design.

7. STRUCTURAL ANALYSIS

A structural analysis will provide the limits of operation of the turbine, in terms of rotational speed, in order to prevent structural failure. The analysis is done as follows:

- A configuration of the wind structure is proposed.
- The maximum bending moment, normal and shear loads on a blade are analyzed.
- Consulting tables of mechanical properties of materials, the ultimate stress modules are found.
- The allowable stresses and loads are calculated using a safety factor.
- The moment of inertia of the blade shape is found using a CAD program.
- The numeric values of the allowable loads are calculated.
- A check is done to see if the turbine is able to accelerate to a point where the structural allowable limits can be surpassed.

7.1 Rotor configuration

Three different rotor configurations (see figure 20) have been tested and are presented in the following figure, they have been numbered from left to right in order to refer them further in the analysis.

The first configuration attaches each blade by two points, which correspond to the Bessel points and minimize the maximum bending moment. These points are located at 20.7% of the blade length from each blade tip; a procedure for obtaining these points by static analysis can be found at (Saranpää, 2010).
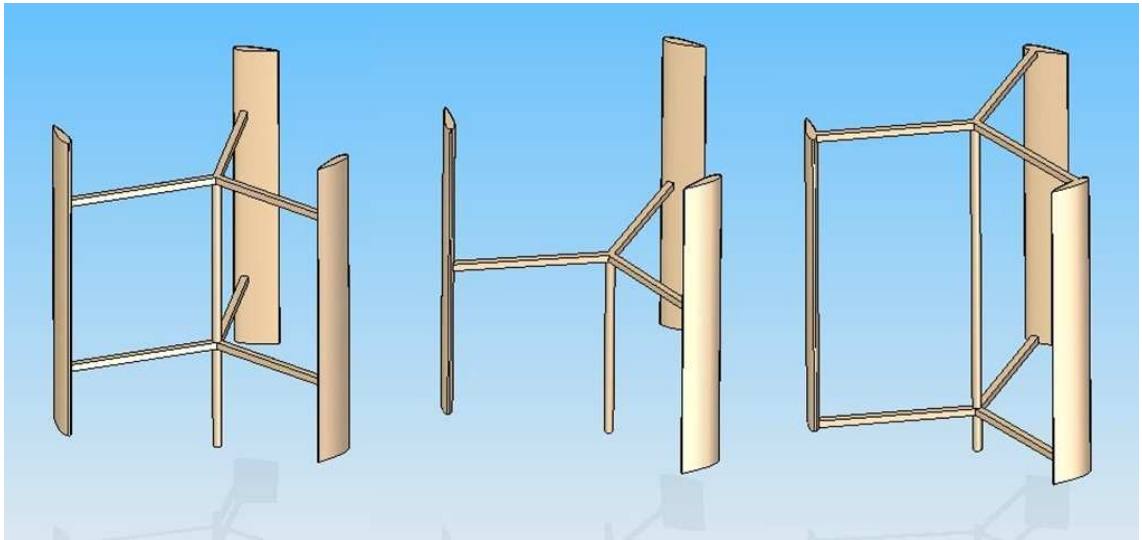
Figure 20. Rotor configurations analyzed.

The second and third configuration are equivalent in terms of maximum bending strength and shear strength, so the third rotor configuration is discarded as the second has lower exposed area per same strength, which will reduce the resulting drag associated with central mast and struts.

7.2 Allowable stress and selected materials

The allowable stress is defined as:

$$Allowable\ stress = \frac{Yield\ or\ Ultimate\ strength}{Factor\ of\ safety} \qquad [7.1]$$

with a factor of safety bigger than 1 if the structure has to avoid failure. For brittle materials such as concrete or materials without a defined yield strength, like wood, the ultimate strength instead the yield stress is used.

The ultimate strength is dependent on the material used; in this design, the chosen material is wood for blades, beams and mast. The type of wood has to be determined according to the local availability in each region.

General guidelines for choosing an appropriate wood are:

- Lightweight softwood is the most suitable and heartwood is more appropriate than sapwood (Piggot, 2001).
- It should be free from knots. Knots introduce discontinuities which lower the mechanical properties, having a greater effect in axial tension than in axial compression so they should be orientated in order to stand compression loads (Forest Products Laboratory, 2010, p. 5.28).
- The grain should run parallel as possible to the longitudinal axis.

Wood selection has been done regardless of wood availability in the country of destination; three different types of wood had been considered in order to have wider range of manufacturing possibilities. Final dimensions will then be function of the type of wood used for the construction of the model. The strength data of these species can be found on appendix 7.

- Sitka spruce (*Picea sitchensis*) has been by far the most important wood for aircraft construction and, although it may not be readily available, its properties can be taken as reference in order to find technically similar woods.
- Balsa (*Ochroma pyramidale*) wood is widely distributed throughout tropical America from southern Mexico to southern Brazil and Bolivia, it has been included in the analysis because is the lightest and softest of all woods on the market (Forest Products Laboratory, 2010, p. 36).
- Obeche (*Triplochiton scleroxylon*), original from west-central African area is a hardwood type wood that can be found in some retail shops so it has been included for a possible prototype candidate.

In order to determine which factor of safety should be applicable, this data has been considered:

- Compression parallel to grain has an average coefficient of variation of 18%.
- Shear parallel to grain has an average coefficient of variation of 14%.

As an average value, a factor of safety of 1.5 will be considered in first place in order to absorb the possible inaccuracies in the load calculation, the variability of the material used or the deterioration due to atmospheric conditions.

Once the allowable stress is calculated, the allowable load is calculated with (Gere, 2004):

$$Allowable\_load = Area \; Allowable\_stress \qquad [7.2]$$

Figure 21 presents the maximum allowable loads for bending moment as a function of the blade material and rotor configuration.
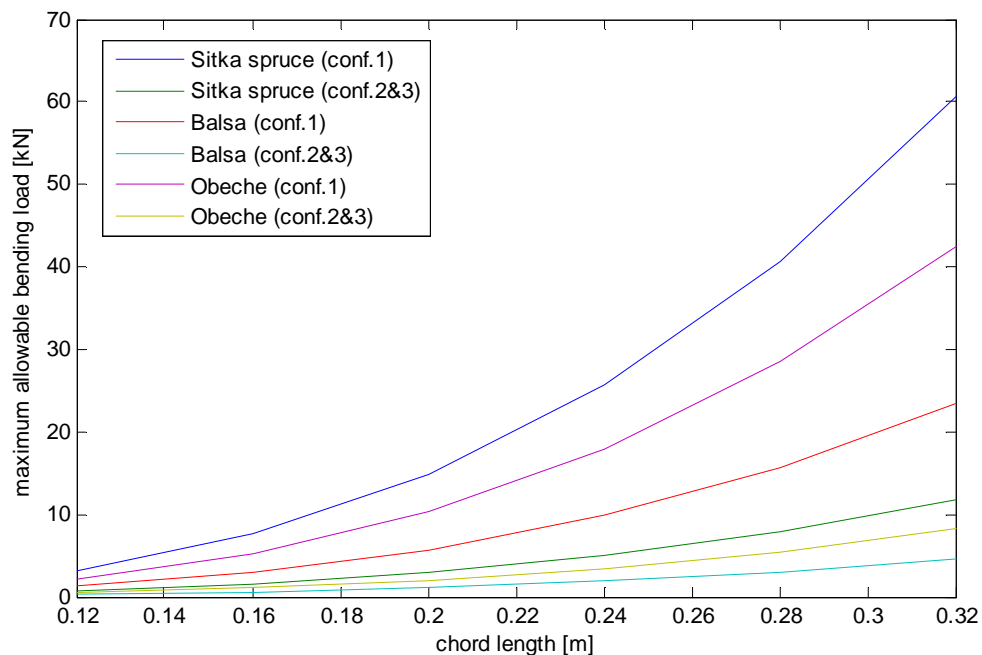
Figure 21. Maximum allowable bending load depending on chord length, blade material and rotor configuration.

We can appreciate a big difference in rotor strength between rotor configuration one and the others, second and third configurations are not further considered in the analysis as the limitation in maximum load relates directly with the maximum tip speed ratio and thus power coefficient.

Wood blades structural strength are limited by the bending moment strength rather than their shear stress as can be appreciated in maximum strength calculations from Table 11 in appendix 7. The values of blade maximum allowable bending load for the first rotor configuration using different woods are found on Table 13 from appendix 7.

7.3 Load analysis

The loads analyzed for the blade dimensioning are divided into centrifugal and aerodynamic loads. The centrifugal force is dependent on both radius and the square of the rotational speed.

$$F_c = m\,R\,\omega^2 \qquad\qquad [7.3]$$

where Fc is the centrifugal force [N], m is the blade mass [kg], R is the rotor radius [m] and ω the rotational speed [rad/s].

The normal force Fn is the aerodynamic load, an analysis of the resultant of the normal force and centrifugal force is made for one blade in a revolution. As they have equal direction, their resultant is:

$$F_r = F_c + F_n \qquad\qquad [7.4]$$

Knowing the maximum allowable load for a given blade chord and a given material, the maximum rpm for each rotor construction can be found. The aerodynamic load is considered to be the load produced when the turbine achieves its cut-out speed, which has been deduced from the average value found on appendix 4 and corresponds to 25 m/s.

The maximum allowable loads, as well as blade mass and maximum rpm are found on tables, we can establish the structural limit of the wind turbine at 580 rpm and 25 m/s wind speed regardless of blade material considering a blade chord of 0.28 m.

8. FINAL DESIGN AND OPERATION

With all the previous considerations, keeping in mind that a prototype must be built in order to validate the algorithm results and possibly make further refinements, the candidate for a prototype is presented on table 6

Symbol	Parameter	Value
Vci	Cut-in windspeed	4 m/s
Vrs	Rated windspeed	9 m/s
Vco	Cut-out windspeed	25 m/s
TSR	Optimum tip speed ratio	2.8
Cp	Maximum power coefficient	0.45
R	Rotor radius	1 m
c	Blade chord	0.28 m
L	Blade length	2 m
N	Number of blades	3
α_o	Initial angle of attack	0^0

It's power curve has been predicted graphically according to the procedure stated at Manwell, McGowan and Rogers (2009, p. 336-340) assuming a generator efficiency of 0.85; the procedure consists in matching the power output from the rotor as a function of wind and rotational speed (see next figure) and with their data make a Power output versus wind speed plot.
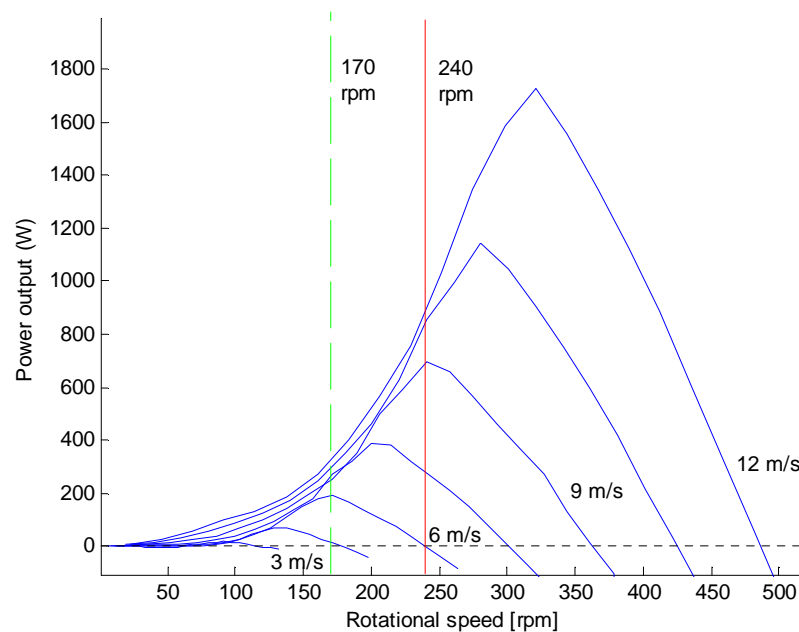
Figure 22. Power output at several rotational and wind speeds. A generator efficiency of 0.85 is assumed.

The rotor design gives (theoretically) 690 W at rated wind speed and the power obtained at 6 m/s at the same rotational speed is almost 0. Nevertheless, the power prediction curve should be made with field test data, as the generator specifications, algorithm inaccuracies and control system used play an important role on the shape of the power curve.

The rotor torque curves at different rotational and wind speeds are presented on next figure.
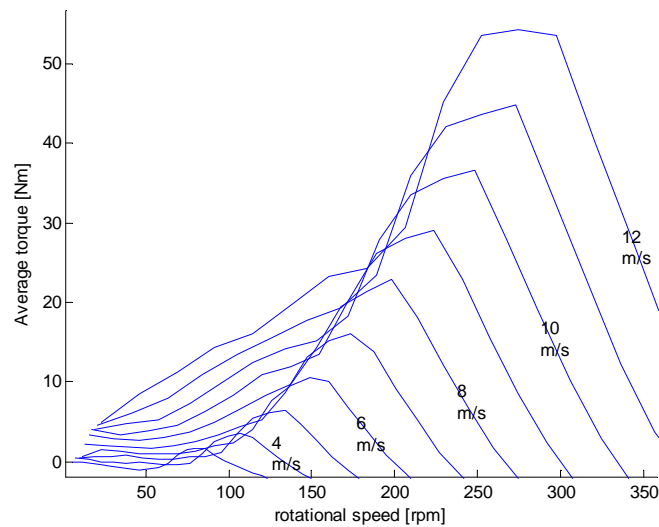
Figure 23. Average torque curves for several wind and rotational speeds.

A mechanism to mechanically stop the wind turbine before the structural limit is surpassed has to be designed. In HAWT models, the over speed control is achieved turning away the frontal area of the turbine from the wind direction or changing the blade pitch (angle of attack) in order to stall the blades. These mechanisms may present spring-loaded devices, and although a fixed pitch was considered for the initial design, perhaps a furling mechanism of the rotor blades when certain centrifugal force is achieved can be considered in the design.

9. CONCLUSIONS

Wood is a suitable material for blade construction in small-scale wind turbines and the construction of an affordable wind turbine with common workshop tools can be contemplated.

A three-bladed design is more efficient than a four-bladed rotor; a low solidity wind turbine may present self-starting problems as rotor efficiency is poor at low tip speed ratios.

There is an optimum turbine rotational speed for each ambient wind speed at which the maximum efficiency is achieved. The energy production of a fixed-pitch wind turbine can be improved adjusting the rated airspeed to the place of installation average wind conditions in order to reach its maximum efficiency.

Larger radius turbines are more efficient than small turbines at same rotational speed as the tangential airspeed increase leads to smaller angles of attack, bigger Reynolds numbers and thus bigger blade lift coefficients.

Experimental tests are needed in order to refine the design and validate the aerodynamic model used.

10. BIBLIOGRAPHY

Abbott, I. H., & Von Doenhoff, A. E. (1959). *Theory of Wing Sections Including a Summary of Airfoil Data.* New York: Dover Publications, Inc.

Aerospaceweb.org. (2005). Retrieved 10 29, 2011, from http://www.aerospaceweb.org/design/scripts/atmosphere/

allsmallwindturbines.com. (2011). Retrieved September 2011, from allsmallwindturbines.com: http://www.allsmallwindturbines.com/

American Wind Energy Association. (2002). *The U.S. Small Wind Turbine Industry Roadmap.* Retrieved September 2011, from American Wind Energy Association: http://www.awea.org/learnabout/smallwind/upload/US_Turbine_RoadMap.pdf

Blackwell, B. F., & Reis, G. E. (1974). *Blade Shape for a Troposkien Type of Vertical-Axis Wind Turbine.* Sandia Laboratories.

Brahimi, M. T., Allet, A., & Paraschivoiu, I. (1995). Aerodynamic Analysis Models for Vertical-Axis Wind Turbines. *International Journal of Rotating Machinery* , Vol.2 No. 1 pp. 15-21.

Cace, J., ter Horst, E., Syngellakis, K., Maíte, N., Clement, P., Heppener, R., et al. (2007). *Urban windturbines, guidelines for small wind turbines in the built environment.* Retrieved September 2011, from Urbanwind.org: http://www.urban-wind.org/pdf/SMALL_WIND_TURBINES_GUIDE_final.pdf

Claessens, M. C. (2006). *The Design and Testing of Airfoils for Application in Small Vertical Axis Wind Turbines.* Delft: Delft University of Technology-Faculty of Aerospace Engineering.

Cooper, P. (2010). Development and analysis of vertical-axis wind turbines. In W. Tong, *Wind power generation and wind turbine design* (pp. 289-296). WIT Press.

Cheikhrouhou, H. (2011). *Energy and Power*. Retrieved September 2011, from African Development Bank Group: http://www.afdb.org/en/topics-and-sectors/sectors/energy-power/

Dunnett, S. (n.d.). *Small wind energy systems for battery charging.* Retrieved September 2011, from Practical Action: http://practicalaction.org/docs/energy/wind_energy_battery_charging.pdf

Encraft. (2009). *Encraft Warwick Wind Trials Project*. Retrieved September 2011, from http://www.warwickwindtrials.org.uk/resources/Warwick+Wind+Trials+Final+Report+.pdf

Forest Products Laboratory. (2010). *Wood handbook, wood as an engineering material.* Madison: United States Department of Agriculture.

Gere, J. M. (2004). *Mechanics of materials.* Brooks/Cole-Thomson Learning.

Jha, A. R. (2011). *Wind Turbine Technology.* New York: CRC Press.

Legros, G., Havet, I., Bruce, N., & Bonjour, S. (2009). *The Energy Acces Situation in Developing Countries.* New York: UNDP and World Health Organization.

Manwell, J. F., McGowan, J. C., & Rogers, A. L. (2009). *Wind Energy Explained - Theory, Design and Application.* John Wiley & Sons Ltd.

Paraschivoiu, I. (2002). *Wind Turbine Design With Emphasis on Darrieus Concept.* Presses internationales Polytechnique.

Paraschivoiu, I., Trifu, O., & Saeed, F. (2009). H-Darrieus Wind Turbine with Blade Pitch Control. *International Journal of Rotating Machinery* , Article ID 505343.

Piggot, H. (2001). *Windpower workshop.* Centre for Alternative Technology.

Raciti Castelli, M., Englaro, A., & Benini, E. (2011). The Darrieus wind turbine: Proposal for a new performance prediction model based on CFD. *Elsevier Energy* , 4919-4935.

Saranpää, O. (2010). *Painerungon osien kuljetuskehikoiden analysointi ja kehittäminen.* Tampere: Opinnäytetyö (Thesis).

Sheldahl, R. E., & Klimas, P. C. (1981). *Aerodynamic Characteristics of Seven Symmetrical Airfoil Section Trough 180-Degree Angle of Attack for Use in Aerodynamic Analysis of Vertical Axis Wind Turbines.* Albuquerque: Sandia National Laboratories.

Spera, D. (2009). *Wind Turbine Technology, fundamental concepts of wind turbine engineering.* ASME Press.

Talayero, & Telmo. (2008). *Energía eólica.* Zaragoza: Prensas universitarias de zaragoza.

Tong, W. (2010). Fundamentals of wind energy. In W. Tong, *Wind power generation and wind turbine design* (p. 112). WIT Press.

Tullis, S., Fiedler, A., McLaren, K., & Ziada, S. *Medium-solidity Vertical Axis Wind Turbines for use in Urban Environments.* Hamilton, Canada.

U.S. Energy Information Administration. (2011, March). *U.S. Department of Energy*. Retrieved November 2011, from http://www.eia.gov/oiaf/aeo/tablebrowser/#release=IEO2011&subject=1-IEO2011&table=2-IEO2011&region=0-0&cases=Reference-0504a_1630

Wahl, M. (2007). *Designing an H-rotor type Wind Turbine for Operation on Amundsen-Scott South Pole Station.* Uppsala: Uppsala Universitet.

winafrique. (2011). Retrieved September 2011, from winafrique.com: http://www.winafrique.com/index.php?option=com_content&view=article&id=92&Itemid=145

Windfinder. (2011). Retrieved September 2011, from Windfinder.com: http://www.windfinder.com/windstats/windstatistic_pyhajarvi_tampere.htm

Wood, D. (2011). *Small Wind Turbines – Analysis, Design, and Application.* Springer-Verlag.

APPENDIXES

SYMBOLS   APPENDIX 1

ad, au	downstream and upstream interference factors
c	blade chord
Cd	drag coefficient
Cl	lift coefficient
Cn	normal coefficient
Cp, Cpd, Cpu	power coefficient, downstream and upstream
Cqav	average torque coefficient
Ct	tangential coefficient
Fc	centrifugal force
Fn	normal force
Fr	resultant force
Ft	tangential force
fup	function characterizing upwind flow conditions
Gb	basic wood specific gravity
GMC	wood specific gravity at MC moisture content
I	inertia moment
Kv	air kinematic viscoity
L	blade length
MC	moisture content
MCft	wood fiber saturation point
N	number of blades
Pw	power available from wind
Q, Qav	torque, average torque
R	rotor radius
Reb	local blade's Reynolds number
S	swept area
SMC	wood volumetric percent shrinkage at MC moisture content
So	wood volumetric percent shrinkage from green to ovendry
TSR	tip speed ratio
W, Wu	resultant air velocity
Vd	downstream induced velocity
Ve	equilibrium-induced velocity
Vo	ambient airspeed
Vu	upstream induced velocity
Xt	rotor tip speed ratio
α	angle of attack/angular acceleration
αo	initial angle of attack
θ	angle between Vo and the position of the blade in the rotor
ρ	air density
ρMC	wood density at x moisture content
ρw	water density at 4℃
σ	solidity
ω	rotor angular speed

Compressive strength parallel to grain: Maximum stress sustained by a compression parallel-to-grain specimen having a ratio of length to least dimension of less than 11 (Definition taken from (Forest Products Laboratory, 2010)).

Cut-in windspeed: The minimum windspeed at which the wind turbine starts producing energy.

Cut-out windspeed: The maximum windspeed at which the wind turbine stops operating, mainly for safety reasons.

NACA-series Airfoil: an airfoil which section and aerodynamic properties are available in reference books like Abbott & Von Doenhoff, 1959, these airfoil data are the result of the research conducted at the National Advisory Commite for Aeronautics (NACA).

Rated windspeed: windspeed at which the rated power is produced, this value defines the shape of the power curve.

Shear strength parallel to grain: Ability to resist internal slipping of one part upon another along the grain. (Definition taken from (Forest Products Laboratory, 2010).

Troposkien shape: is a word derived from the Greek, means turning rope and is used to describe the shape assumed by a cable if its ends are attached to two points and it is spun at constant angular velocity (Blackwell & Reis, 1974). This shape is used to minimize the bending stress in the blades of Darrieus turbines.
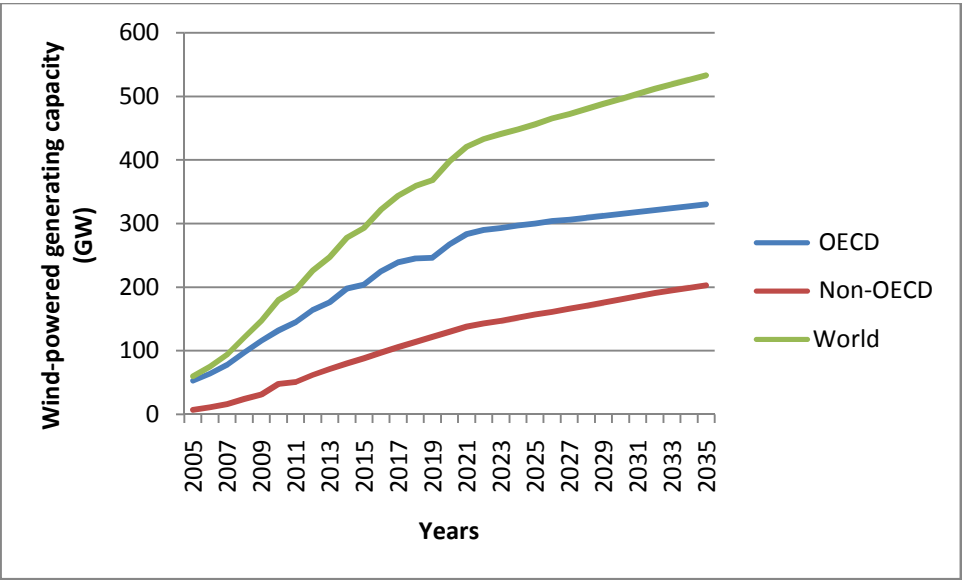
Figure 24. World wind-powered generating capacity trend (U.S. Energy Information Administration, 2011)
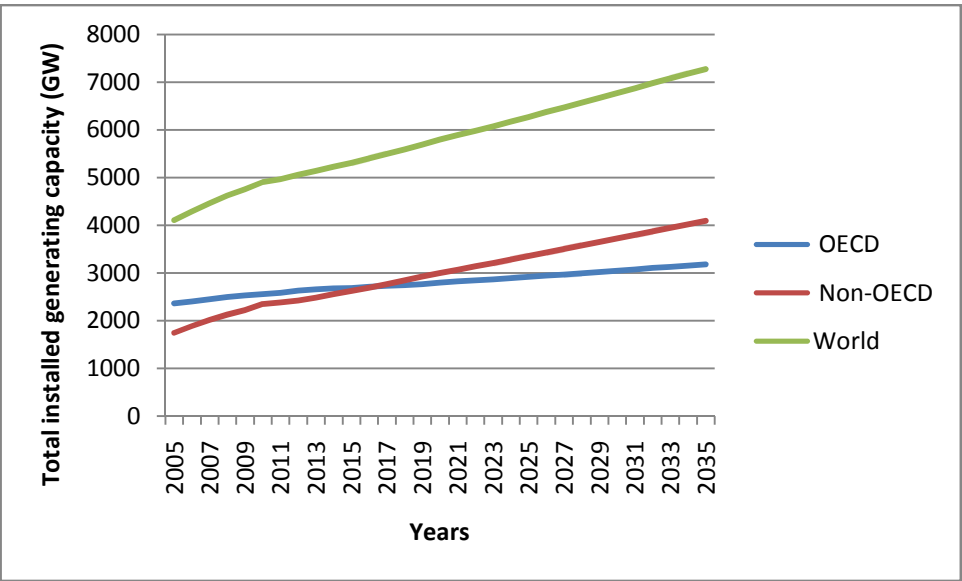
Figure 25. World total installed generating capacity trend (U.S. Energy Information Administration, 2011)

COMPETENCE ANALYSIS

Table 7. Market turbines analysis (1)

Product	Manufacturer	Rated Power (W)	Rated Wind Speed (m/s)	Rated rpm	N	Price €
Turby		2500	14	120/400	3	11466
Windspire	Windspire Energy, US	1200	10,7		3	11354
P-1000	Shanghai Aeolus Windpower	1000	12		5	2826
Easy Vertical	Ropatec	1000	12	240	3	
FL1KWVAWT	Flexienergy	1000	10	55		
Windterra Eco 1200	Windterra systems	1000	11	270 max	3	
VENCO-Twister 1000 T	VENCO Power GmbH	1000	12		3	
Mini Vertical	Ropatec	750	14	180	3	
Aeolos-V 600w	Aeolos Wind Turbine	600	10			
P-500	Shanghai Aeolus Wind-power	500	13		5	1680
FSW Gyro.5	Four Seasons Windpower	500	10,72		5	1949
Seahawk 500	Wepower	500	12,5	608	6	
FLEX500VAWT	Flexienergy	500	13			
FSW Gyro.3	Four Seasons Windpower	300	9,92		5	1383
Aeolos-V 300w	Aeolos Wind Turbine	300	10			
VENCO-Twister 300 T	VENCO Power GmbH	300	14		3	
FSW Gyro.2	Four Seasons Windpower	200	9,92		5	1207
Wind Smile 200W	Wind Smile	200	13		4	
ELY-100	Qingdao	100	10	200	5	

COMPETENCE ANALYSIS   APPENDIX 4: 2(2)

Table 8. Market turbine analysis (2)

Product	Blade Lenght (m)	Rotor radius (m)	Swept Area (m^2)	Total Height (m)	Min Wind (m/s)	Max Wind (m/s)	Survival Wind (m/s)	Calc. Cp
Turby	2,6	1,9	9,88		4	14	55	0,15
Windspire	5,79	0,61	7,06	9,1	3,8		47	0,23
P-1000	2	0,9	3,60	5,5	4	25	50	0,26
Easy Vertical	1,9	0,95	3,61	6,8	3		53	0,26
FL1KWVAWT	1,65	1,25	4,13	8	3	25	40	0,40
Windterra Eco 1200	2,66	1,125	5,99		3		53	0,20
VENCO-Twister 1000 T	1,9	0,95	3,61		3,5	20	50	0,26
Mini Vertical	1,5	1,5	4,50		3		53	0,10
Aeolos-V 600w	1,6	0,65	2,08		2		50	0,47
P-500	1,05	0,68	1,43	5,5	4	25	45	0,26
FSW Gyro.5	2,21	0,68	3,01	5,49	1,96	24,6	40,2	0,22
Seahawk 500	1,2	0,381	0,91		1,35		54	0,46
FLEX500VAWT	1	0,6	1,20		4,5			0,31
FSW Gyro.3	1,29	0,68	1,75	5,49	1,96	24,6	40,2	0,29
Aeolos-V 300w	1,4	0,6	1,68		2		50	0,29
VENCO-Twister 300 T	1	0,5	1,00		3,5	25	50	0,18
FSW Gyro.2	0,89	0,68	1,21	5,49	1,96	24,6	40,2	0,28
Wind Smile 200W	1	0,5	1,00	1,4	2,5		60	0,15
ELY-100	0,8	0,8	1,28	6	1,5	25	50	0,13

```
%This function calculates the power coefficient and average torque
%for a vertical axis wind turbine according to the procedure stated at:
%"Double-Multiple Streamtube model for Darrieus wind turbines,
%I.Paraschivoiu", the equations have been adapted to a straight bladed
%wind turbine when necessary.


%function [Cpt, av_T] = f_Cp_and_av_T2 (Vo, w, R, N, c, L, Ao, NACA)


%%INPUT PARAMETERS
%Vo = ambient air speed (m/s).
%w = rotor angular speed (rad/s).
%R = rotor radius (m).
%N = number of blades.
%c = blade chord (m).
%L = blade length (m).
%Ao = initial angle of attack (rad).
%NACA = airfoil used (15 or 21).


%%OUTPUT PARAMETERS
%Cpt = power coefficient.
%av_T = average torque (Nm).


%%CONSTANTS FOR STANDARD AIR CONDITIONS AND SEA LEVEL
kv = 1.4607e-5;       % Kinematic viscosity at 15ºC [m^2/s].
rho = 1.225;          % air density (Standard density at sea level)[kg/m^3]


%%OTHER PARAMETERS
n=36;    % number of streamtubes (180/5) divides one half of the rotor in 5º
         % increments.


% theta = vector containing the angles between streamtube and local radius
% to the rotor axis.
thetau = linspace (-89*pi/180, 89*pi/180, n); % upstream angles (rad).
thetad = linspace (91*pi/180, 269*pi/180, n); % downstream angles (rad).


Xt = w*R/Vo;      %Tip speed ratio
```

```matlab
S = 2*L*R;        %Swept area [m^2]



%%-------------- UPSTREAM CALCULATION --------------------
%%Get the corresponding au value for each streamtube (each theta value)


i = 0;                       %initialize the counter value
while (i~=n)
    i = i+1;
    au = 1.01;               % velocity induction factor upstream.
    newau = 1;               % initialize, au must be different from newau


    while ((au-newau)>1e-3)      %Iterative process to find au
        au = newau;
        Vu = Vo*(au);   %Vu =velocity upstream of wind turbine cylinder


        X = R*w/Vu;     %Local Tip speed ratio


        % Wu=local resultant air velocity
        Wu = sqrt ( Vu^2*( (X - sin (thetau(i)))^2 + (cos (thetau(i)))^2));


        Reb = Wu*c/kv; %Blade Reynolds number


        % the values from airfoil lift and drag coefficients depending on
        % the angle of attack are interpolated for the given Reynolds num-
        % ber
        if (NACA==15)
                [A1, Cl1, Cd1] = NACAfinder15 (Reb); %NACA0015
        else
                [A1, Cl1, Cd1] = NACAfinder21 (Reb); %NACA0021
        end


        costh = cos(thetau(i));
        cosao = cos(Ao);
        sinth = sin(thetau(i));
        sinao = sin(Ao);
        A = asin((costh*cosao-(X-sinth)*sinao)/sqrt((X-sinth)^2+(costh^2)));
```

```matlab
% if angle of attack is negative the sign is changed for interpola-
% ting in the data tables and then the lift coefficient sign is
% changed.
neg = 0;
if (sign(A)==-1)
    neg = 1;
end


A = abs(A*180/pi); %Conversion to degrees to match table
Cl = interp1 (A1, Cl1, A, 'linear');
Cd = interp1 (A1, Cd1, A, 'linear');


if (neg==1)
        A = -1*A; %Restablish the original value for plots
        Cl =-1*Cl;
        Cd =1*Cd;
end


% Cn = normal coefficient, % Ct = tangential coefficient
Cnu = Cl*cosd (A) + Cd*sind (A); %note that A is in degrees
Ctu = Cl*sind (A) - Cd*cosd (A);



% fup = function to find interference factor (au).
g=@(thetau) (abs(sec (thetau)).*(Cnu.*cos(thetau)-
Ctu.*sin(thetau)).*(Wu./Vu).^2);
y = quadl (g, -89*pi/180, 89*pi/180);
fup = N*c*y/(8*pi*R);


%[newau] = solve ('fup*newau = pi*(1-newau)')
%syms newau
%S1 = solve ('fup*newau*R = pi*(1-newau)*r(k)', 'newau')


newau = pi/(fup+pi);    % new interference factor value for the next
                        % iteration process.
        end
```

```matlab
        Auvector (i) = A;           % Store angle of attack value

        auvector (i) = newau;       % Store au value in a vector


        Fnu (i) = (c*L/S)*Cnu*(Wu/Vo)^2;  % normal force coefficient

        Ftu (i) = (c*L/S)*Ctu*(Wu/Vo)^2;  % tangential force coefficient

        Tup (i) = 0.5*rho*c*R*L*Ctu*Wu^2; % torque produced in when the blade

                                          % crosses this streamtube



    end



    % Average upstream torque
    ts2 = f_trapezoidal_integration_s (thetau, Tup)

    av_Tup = N*(ts2)/(2*pi)            %upstream average torque


    % Average torque coefficient
    av_Cqu = av_Tup/(0.5*rho*S*R*Vo^2)

    Cpu = av_Cqu*Xt;                   %upstream power coefficient



    %%--------------- DOWNSTREAM CALCULATION --------------------



    j = n+1;
    flag =0;
    i = 0;                     %initialize the counter value
    while (j~=1)
        j = j-1;
        i = i+1;               % interference factor downstream.
        ad = 1.01;             % velocity induction factor upstream.
        newad = auvector(j);   % initialize, au must be different from newau


        while ((ad-newad)>1e-3)      %Iterative process to find ad
            ad = newad;
            Ve = Vo*((2*auvector(j))-1);    %Ve = air velocity inside cylinder

            Vd = Ve*ad;      %Vd = air velocity downstream of cylinder

            X = R*w/Vd;      %Local Tip speed ratio


            % Wd=local resultant air velocity
```

```
Wd = sqrt ( Vd^2*( (X - sin (thetad(i)))^2 + (cos (thetad(i)))^2));

Reb = Wd*c/kv; %Reynolds number of the blade

if (NACA==15)

        [A1, Cl1, Cd1] = NACAfinder15 (Reb);

else

        [A1, Cl1, Cd1] = NACAfinder21 (Reb);

end


costh = cos(thetad(i));

cosao = cos(Ao);

sinth = sin(thetad(i));

sinao = sin(Ao);

A = asin((costh*cosao-(X-sinth)*sinao)/sqrt((X-sinth)^2+(costh^2)));


neg = 0;

if (sign(A)==-1)

    neg = 1;

end


A = abs(A*180/pi); %Conversion to degrees to match table

Cl = interp1 (A1, Cl1, A, 'linear');

Cd = interp1 (A1, Cd1, A, 'linear');


if (neg==1)

        A = -1*A; %Restablish the original value for plots

        Cl =-1*Cl;

        Cd =1*Cd;

end

% Cn = normal coefficient, % Ct = tangential coefficient

Cnd = Cl*cosd (A) + Cd*sind (A); %note that A is in degrees

Ctd = Cl*sind (A) - Cd*cosd (A);


    g=@(thetad) (abs(sec (thetad)).*(Cnd.*cos(thetad)-
Ctd.*sin(thetad)).*(Wd./Vd).^2);

    y = quadl (g, 91*pi/180, 269*pi/180);

    fdw = N*c*y/(8*pi*R);

    %[newau] = solve ('fup*newau = pi*(1-newau)')
```

```matlab
        %syms newau

        %S1 = solve ('fup*newau*R = pi*(1-newau)*r(k)', 'newau')

        if (flag ==0)

            newad = pi/(fdw+pi);

        end


        %if the iteration process does not converge, the value of the

        %interference factor upstream from the same streamtube is taken

        if (newad<0.01)

            warning('newad<0.01 at theta = %d and A = %d', (thetad(i)*180/pi),
A);

            if (i>1)

                newad = advector(i-1);

            else

                newad = auvector (i);

            end

                flag = 1;

        end

    end


    Advector (i) = A;

    advector (i) = newad;    %Store ad value in a vector


    % Force coefficients and torque calculation

    Fnd (i) = (c*L/S)*Cnd*(Wd/Vo)^2;

    Ftd (i) = (c*L/S)*Ctd*(Wd/Vo)^2;

    Tdw (i) = 0.5*rho*c*R*L*Ctd*Wd^2;

end


% Average upstream torque

ts4 = f_trapezoidal_integration_s (thetad, Tdw)

av_Tdw = N*(ts4)/(2*pi)              % upstream average torque


% Average torque coefficient

av_Cqd = av_Tdw/(0.5*rho*S*R*Vo^2)


Cpd = av_Cqd*Xt;                     % downstream power coefficient
```

```
Cpt = Cpd+Cpu              % Total power coefficient

av_T = av_Tup + av_Tdw     % Total average torque [Nm]
```

NACA0021 AIRFOIL DIMENSIONS   APPENDIX 6

Table 9. NACA0021 airfoil ordinates and measures.

Ordinates		chord	28 cm
x(%c)	y(%c)	x	y
0	0,000	0	0
1,25	3,315	0,35	0,9282
2,5	4,576	0,7	1,2813
5	6,221	1,4	1,7419
7,5	7,350	2,1	2,058
10	8,195	2,8	2,2946
15	9,354	4,2	2,6191
20	10,040	5,6	2,8112
25	10,397	7	2,9112
30	10,504	8,4	2,9411
40	10,156	11,2	2,8437
50	9,265	14	2,5942
60	7,986	16,8	2,2361
70	6,412	19,6	1,7954
80	4,591	22,4	1,2855
90	2,534	25,2	0,7095
95	1,412	26,6	0,3954
100	0,221	28	0,0619
L.E. radius (%c)		4,85	

WOOD PROPERTIES AND STRUCTURAL STRENGTHS   APPENDIX 7

Table 10. Wood properties (Forest Products Laboratory, 2010)

Timber type	Sitka Spruce (*Picea sitchensis*)	Balsa (*Ochroma pyramidale*)	Obeche (*Triplochiton scleroxylon*)
Basic Specific gravity	0.40	0.16	0.3
Volumetric Shrinkage from green to ovendry moisture content [%]	11.5	10.8	9.2
Calculated density at 19% moisture content [kg/m3]	496.95	198.25	369.46
Compression parallel to grain [kPa]	38700	14900	27100
Shear parallel to grain [kPa]	7900	2100	6800
Average parallel to grain tensile strength [kPa]	59300		
Modulus of Elasticity [MPa]	10800	3400	5900
Modulus of rupture [kPa]	70000	21600	51000

The wood density (included on table 9) varies in function of moisture content, having the specific gravity of the wood and the moisture content MC, the density is calculated using the procedure stated at (Forest Products Laboratory, 2010):

$$\rho_{MC} = \rho_w \, G_{MC}(1 + \frac{MC}{100})$$ [1.1]

where ρ_w is the water density at 4℃ which is considered to be (1000 kg/m^3), x is the moisture content in % and Gx is the specific gravity at the given moisture content, which is calculated using:

$$G_{MC} = G_b/(1 - \frac{S_{MC}}{100})$$ [1.2]

where G_b is the basic specific gravity and S_x is calculated using:

$$S_{MC} = S_o \left(1 - \frac{MC}{MC_{ft}}\right)$$ [1.3]

where MC_{ft} is the fiber saturation point taken as 30% when unknown and S_o is the wood volumetric percent shrinkage from the green condition to ovendry which depends on wood type and its value is found at (Forest Products Laboratory, 2010, pág. 4.8), the moisture content will be assumed to be 19% which is the value of moisture content at which wood is considered dry by the American Softwood Lumber Standard (Forest Products Laboratory, 2010, pág. 6.18).

Table 11. Maximum bending moment and shear stress for the three rotor configurations

	Maximum Bending moment	Maximum Shear Stress
First	$q\ \dfrac{(L_1)^2}{2}$	$q\ L_1$
Second	$q\ \dfrac{L^2}{8}$	$q\ \dfrac{L}{2}$
Third	$q\ \dfrac{L^2}{8}$	$q\ \dfrac{L}{2}$

Table 12. Airfoil geometric properties for use in the structural calculations.

Blade airfoil geometric properties used to predict blade stresses					
Chord length [m]	0,16	0,2	0,24	0,28	0,32
Total Area [mm]^2:	3682,3	5753,59	8285,17	11277,04	14729,19
Centroid X [mm]:	67,25	84,06	100,87	117,69	134,5
Centroid Y [mm]:	0	0	0	0	0
Area Moment of Inertia in X (Ixx) [mm^4]:	239204,84	583996,18	1210974,48	2243479,73	3827277,37
Area Moment of Inertia in Y (Iyy) [mm^4]:	5198450,12	12691528,62	26317153,75	48755776,35	83175201,98
Upper half blade airfoil geometric properties					
Area [mm]^2:	1841,15	2876,79	4142,58	5638,52	7364,59
Centroid X [mm]:	67,25	84,06	100,87	117,69	134,5
Centroid Y [mm]:	6,75	8,44	10,13	11,82	13,51
Area Moment of Inertia in (Ixx) [mm^4]:	35597,2	86907,23	180210,83	333862,81	569555,21
Area Moment of Inertia in (Iyy) [mm^4]:	2599225,06	6345764,31	13158576,88	24377888,18	41587600,99

Table 13. Rotor blade limits depending on construction material.

	Sitka spruce	Obeche	Balsa
Maximum allowable bending load [kN]	45.95	32.17	17.69
Blade mass [kg]	11.2	8.33	4.47
Maximum revolutions [rpm]	604.15	582.85	583.47